

POLITECNICO DI TORINO

Corso di Laurea Magistrale in Ingegneria Elettrica



Tesi di Laurea Magistrale

Modeling active distribution networks in real time

Supervisors

Prof. Andrea MAZZA

Prof. Ettore BOMPARD

Ing. Giorgio BENEDETTO

Candidate

Matteo BECHIS

November 2024

Abstract

The rise of Renewable Energy Sources (RES) connected to the distribution system, either alongside or replacing traditional turbine-generator power plants, is leading to Low-Inertia Power Systems. These systems require the development of innovative solutions to effectively manage frequency stability. The Real Time Simulation (RTS) is a fundamental tool for testing and enhancing strategies and hardware solutions before their implementation on the field.

This work examines the various aspects of implementing a RTS for a distribution electrical grid, covering from the theoretical foundations of simulations to the practical application of a model using an OPAL-RT simulator. Modeling a distribution power network poses unique challenges compared to the more commonly simulated transmission grids. This discussion addresses several key issues related to this type of simulations, including the modeling of static converters, implementing a tree topology in the simulator, and choosing appropriate solvers to address the specific simulation challenges associated with this modeling approach.

Key words: Real Time Simulation (RTS), distribution grid, Low-Inertia power system, virtual inertia.

Sommario

L'aumento della generazione da fonti rinnovabili collegata alla rete di distribuzione, a supporto o in sostituzione delle tradizionali centrali con turboalternatori, ha dato origine ai Sistemi Elettrici a Bassa Inerzia. Questi sistemi richiedono lo sviluppo di soluzioni innovative per gestire efficacemente la stabilità della frequenza di rete. Le simulazioni in tempo reale rappresentano uno strumento essenziale per testare e ottimizzare strategie e soluzioni hardware prima della loro implementazione nella rete.

Questo lavoro esplora i vari aspetti legati all'implementazione di una simulazione in tempo reale di una rete elettrica di distribuzione, dalla teoria delle simulazioni matematiche fino all'applicazione pratica di un modello su un simulatore OPAL-RT. Modellare una rete di distribuzione comporta sfide uniche rispetto alla più comune simulazione delle reti di trasmissione. Tra i problemi chiave affrontati ci sono la modellazione dei convertitori statici, l'implementazione di una topologia ad albero sul simulatore e la selezione di risolutori adeguati per gestire le specifiche sfide di simulazione per il modello di rete utilizzato.

Parole chiave: Simulazione in tempo reale, rete di distribuzione, sistema elettrico a bassa inerzia, inerzia virtuale.

*Grazie a tutti voi che mi volete bene:
amici, parenti, Banu, Fabi, Dado, Bat, Mamma e Papà.
Perché il timido bambino che diciotto anni fa
iniziava le elementari è diventato l'uomo che
oggi si laurea attraverso le grandi ricchezze e
possibilità che gli avete donato.
Custodisco ognuno di voi in una parte di me,
con il giusto occhio vi troverete.*

Table of Contents

List of Tables	IX
List of Figures	X
List of Acronyms	XIV
List of Symbols	XVI
1 Introduction to dynamic systems	1
1.1 Dynamic problems formalisation	2
1.2 Dynamic problems resolution: digital simulations	3
1.3 Digital simulations challenges	4
1.3.1 Time step	4
1.3.2 Stiffness	5
1.4 Electrical dynamic systems	6
2 Mathematical tools	9
2.1 Numerical Integration	9
2.1.1 Stiff solvers	11
2.1.2 Euler forward method	11
2.1.3 Euler backward method	13
2.1.4 Trapezoidal rule method	14

2.1.5	Higher order methods	15
2.1.6	Accuracy comparison	16
2.2	Lower-Upper (LU) factorization	16
3	Electrical systems modeling	18
3.1	Nodal approach	18
3.2	State Space (SS) approach	21
4	Real Time Simulation (RTS)	24
4.1	Applications	25
4.2	Hardware setting	27
4.3	Solvers	28
4.3.1	Dommel’s algorithm: Topological approach	29
4.3.2	State Space (SS)	29
4.3.3	State Space Nodal (SSN) approach	30
4.3.4	Phasor Domain: transient simulation	31
4.3.5	Field Programmable Gate Array (FPGA) based	32
4.4	Challenges	33
4.4.1	Time step	34
4.4.2	Stiffness	34
4.4.3	Jitters	35
4.4.4	Non linearities	36
4.5	Performances	37
5	Model presentation	39
5.1	Topology: Rural Net	41
5.2	Dynamic generation	41
5.2.1	Simulink model	42
5.3	Connection elements	44

5.3.1	Simulink model	45
5.4	Loads and distributed generation	45
5.4.1	Simulink model	45
5.5	Battery Energy Storage System	46
5.5.1	Simulink model	47
5.6	Emergency Automatic Control relay	51
5.6.1	Simulink model	51
5.7	Implementation of the simulation in real time	52
5.7.1	Decoupling the distribution network for multi processor Real Time Simulation: SSN solver	53
6	Model simulation	55
6.1	Hardware description	55
6.2	Scenario description	56
6.2.1	Use case	56
6.2.2	Use case implementation	59
6.3	Results presentation	60
6.3.1	Generator response	60
6.3.2	Emergency Automatic Control (EAC) relays action	62
6.3.3	Battery Energy Storage System (BESS) action	63
Test 1	65
Test 2	67
Test 3	69
Test 4	71
6.3.4	Summary of simulation results	73
7	Conclusion and future works	74
	Bibliography	76

List of Tables

3.1	Matrix stamps of the basic DC components.	21
3.2	Resistive companion modeling of dynamic components.	22
4.1	Solvers characteristics summary.	29
4.2	Solvers modeling summary.	37
5.1	Five largest battery storage power plants by storage capacity. . . .	47
5.2	Specifications for operating BESS.	51
6.1	Scope and objective of use case.	57
6.2	Summary of frequency profile obtained.	73

List of Figures

1.1	Digital simulation.	3
1.2	Simulation time scales in power system.	7
1.3	Simulation time step by application.	8
2.1	Numerical integration.	10
2.2	Stability region of trapezoidal method (A-stable).	12
2.3	Stability region of the Euler Forward integration method.	13
2.4	Stability region of the Euler Backward integration method.	14
2.5	Accuracy comparison: (a) magnitude and (b) phase (sourced from the reference [3]).	17
3.1	Algebraic system formation	19
4.1	Real time simulation requisites and other simulation techniques	25
4.2	Types of simulation interaction.	26
4.3	RTS hardware setting.	28
4.4	Dommel's algorithm flow chart.	30
4.5	SSN flow chart.	31
4.6	Jitters summary.	36
4.7	Non linear resistive companion flow chart.	37
4.8	Solvers performance.	38

5.1	Low-inertia Power System [10].	40
5.2	Model's topology: Rural net.	42
5.3	Dynamic generation Simulink model.	43
5.4	Simulink model of the connection elements.	45
5.5	Dynamic ZIP load Simulink model.	46
5.6	BESS general scheme.	48
5.7	BESS Simulink model.	48
5.8	Control strategy of the BESS for providing virtual inertia and primary frequency response.	49
5.9	Recovery control of BESS on State Of Charge (SOC) ranges.	50
5.10	EAC simulink model.	51
5.11	Network model in Simulink.	52
5.12	Organization of the RTS model in Simulink.	53
6.1	Opal-RT simulator architecture [16].	56
6.2	Diagram of use case.	58
6.3	Frequency transient in response to an 8 MW load step, without any measures in place to maintain frequency stability.	61
6.4	Transient in the synchronous generator in response to an 8 MW load step, without any measures in place to maintain frequency stability.	61
6.5	Frequency transient in response to an 8 MW load step, with intervention from the EAC relays on feeders 1,2,5 and 6.	62
6.6	Transient in the synchronous generator in response to an 8 MW load step, with intervention from the EAC relays on feeders 1,2,5 and 6.	63
6.7	BESS installed on the network.	64
6.8	Frequency transient in response to an 8 MW load step, with intervention from the BESS - Test 1.	65
6.9	Transient in the synchronous generator in response to an 8 MW load step, with intervention from the BESS - Test 1.	65
6.10	Action of BESS connected to the network in response to an 8 MW load step - Test 1.	66

6.11	Frequency transient in response to an 8 MW load step, with intervention from the BESS - Test 2.	67
6.12	Transient in the synchronous generator in response to an 8 MW load step, with intervention from the BESS - Test 2.	67
6.13	Action of BESS connected to the network in response to an 8 MW load step - Test 2.	68
6.14	Frequency transient in response to an 8 MW load step, with intervention from the BESS - Test 3.	69
6.15	Transient in the synchronous generator in response to an 8 MW load step, with intervention from the BESS - Test 3.	69
6.16	Action of BESS connected to the network in response to an 8 MW load step - Test 3.	70
6.17	Frequency transient in response to an 8 MW load step, with intervention from the BESS - Test 4.	71
6.18	Transient in the synchronous generator in response to an 8 MW load step, with intervention from the BESS - Test 4.	71
6.19	Action of BESS connected to the network in response to an 8 MW load step - Test 4.	72

List of Acronyms

AC Alternate Current

ARTEMIS Advanced Real-Time Electro-Magnetic Simulator

ATLANTIDE Archivio TeLemAtico per il riferimento Nazionale di reTI di Distribuzione Elettrica

BESS Battery Energy Storage System

COST Commercial off-the-shelf

DC Direct Current

DER Distributed Energy Resources

DG Distributed Generation

DSP Digital Signal Processing

DSO Distribution System Operator

DT Digital Twin

eHS Electric Hardware Solver

EMT Electromagnetic Transient

EAC Emergency Automatic Control

ESS Energy Storage System

FACTS Flexible AC Transmission Systems

FPGA Field Programmable Gate Array

HIL Hardware in the Loop

HV High Voltage

KCL Kirchhoff's Current Law

KVL Kirchhoff's Voltage Law
LTl Linear Time Invariant
LU Lower-Upper
LV Low Voltage
MBD Model Based Design
MV Medium Voltage
ODE Ordinary Differential Equation
PCC Point of Common Coupling
PWM Pulse Width Modulation
RES Renewable Energy Sources
RMS Root Mean Square
ROCOF Rate Of Change Of Frequency
RTS Real Time Simulation
SIL Software in the Loop
SMES Superconducting Magnetic Energy Storage
SOC State Of Charge
SS State Space
SSN State Space Nodal
TSO Transmission System Operator

List of Symbols

λ : matrix eigenvalues

τ : time constant

\mathbf{b} : input's vector of a linear system in matrix form

\mathbf{b}_p : input's vector of a base element

d : distance coordinate along the power line

e : tension as variable

h : simulation time step

i : current as variable

\mathbf{i}_n : vector of known nodal current injections

k : generic constant

t : time as variable

t_0 : start simulation time

t_c : generic time instant

\mathbf{u} : SS input vector

\mathbf{v} : vector of nodal potentials

w : wave's speed

\mathbf{x} : vector of SS system's variable

\mathbf{x}_0 : vector SS system's variable, initial state

\mathbf{y} : output's vector of a linear system in matrix form

z : generic auxiliary variable

\mathbf{z} : generic auxiliary vector

\mathbf{A} : SS system's matrix

B : number of network's branches

\mathbf{B} : SS system's input matrix

C : capacitance value

\mathbf{C} : SS system's output matrix

\mathbf{D} : SS system's feed forward matrix

H : tranfer function (frequency domain analysis)
 I : constant current value
 \underline{I} : phasorial nodal current vector
 J : number of SS variables
 K : number of SS system's input variables
 L : inductance value
 \underline{L} : lower matrix resulting from LU factorisation method
 M : generic size
 N : number of network's nodes
 P : number of output variables
 R : constant resistance value
 T_{fin} : end simulation time
 \underline{U} : upper matrix resulting from LU factorisation method
 V : constant tension value
 \underline{V} :phasorial nodal tension vector
 \underline{Y} : admittance matrix (from nodal method)
 \underline{Y}_p : admittance matrix of a base element (from nodal method)
 \underline{Y}_c : admittance matrix of a cluster (from SSN)
 Z : impedance value

Chapter 1

Introduction to dynamic systems

The term dynamic refers to phenomena that produce time-changing patterns, the characteristics of the pattern at one time being interrelated with those at other times. The term is nearly synonymous with time-evolution or pattern of change. It refers to the unfolding of events in a continuing evolutionary process.

The term dynamic indicates, first, the time-evolutionary phenomena in the world about us, and, second, that part of mathematical science that is used for the representation and analysis of such phenomena. Although there are endless examples of interesting dynamic situations arising in a spectrum of areas the number of corresponding general forms for mathematical representation is relatively small. Most commonly, dynamic systems are represented mathematically in terms of either differential equations¹ (Ordinary Differential Equation (ODE)) or difference equations². These equations provide the structure for representing time linkages among variables. The process of obtaining the representation is often referred to as modeling, and the final product a model. The theory employed in any given model may be well-founded and generally accepted, or it may be based only on one analyst's hypothesized relationships. In general there is no single "correct" model; instead, the degree of detail, the emphasis and the selection of model form must be determined based on the specific application and scope of the analysis.

¹In mathematics, a differential equation is an equation that relates one or more unknown functions and their derivatives.

²In mathematics, a difference equation is an equation containing finite differences of an unknown function.

The use of either differential or difference equations to represent dynamic behavior corresponds, respectively, to whether the behavior is viewed as occurring in continuous or discrete time. Continuous time corresponds to our usual conception, where time is regarded as a continuous variable and is often viewed as flowing smoothly past us. In mathematical terms, continuous time of this sort is quantified in terms of the continuum of real numbers. Dynamic behavior viewed in continuous time is usually described by differential equations, which relate the derivatives of a dynamic variable to its current value. Discrete time consists of an ordered sequence of points rather than a continuum. In terms of applications, it is convenient to introduce this kind of time when events and consequences either occur or are accounted for only at discrete time periods, such as daily, monthly, or yearly (e.g., a population model). Accordingly, dynamic behavior viewed in discrete time is usually described by equations relating the value of a variable at one time to the values at adjacent times. Such equations are called difference equations.

1.1 Dynamic problems formalisation

The term system, as applied to general analysis, was originated as a recognition that meaningful investigation of a particular phenomenon can often only be achieved by explicitly accounting for its environment. Meaningful analysis must consider the entire system and the relations among its components. Accordingly, mathematical models of systems are likely to involve a large number of interrelated variables. The ability to deal effectively with large numbers of interrelated variables is one of the most important characteristics of mathematical system analysis.

There are two main methods for representing sets of interrelations. The first is vector notation, which provides an efficient representation both for computation and for theoretical development. By its very nature, vector notation suppresses detail but allows for its retrieval when required. Moreover, once a situation is cast in this form, the entire array of theoretical results from linear algebra is available for application. Thus, this language is also well matched to mathematical theory. The second technique for representing interrelations between variables is by use of diagrams. In this approach the various components of a system are represented by points or blocks, with connecting lines representing relations between the corresponding components. This representation is exceedingly helpful for visualization of essential structure in many complex situations; however, it lacks the full analytical power of the vector method.

In the analysis of dynamic problems: the differential (or difference) equations provide the element of dynamics and the vector algebra provides the notation for multi variable representation. Indeed the modeling of many engineering problems

gives rise to a system of ODEs, which can be written as in equation 1.1. In the equation $\mathbf{x}(t)$ is the state variable vector and $\mathbf{u}(t)$ is the input vector.

$$\dot{\mathbf{x}}(t) = f(\mathbf{x}(t), \mathbf{u}(t), t) \tag{1.1}$$

1.2 Dynamic problems resolution: digital simulations

The resolution of the dynamic problems emerge into the digital simulations of dynamic systems. Digital simulations are used as a substitute for analog simulations, which are more expensive, complex, and difficult to build and adapt to various test conditions.

Simulations, emulating the reality, aim to predict the behavior of a physical system by numerically integrating its set of equations at each time step (h), using the results from the preceding time step as the starting point. To notice two general aspects characteristic of digital simulations:

- the dynamic phenomenon is represented by its mathematical model, which could be more or less sophisticated;
- the model's differential equations must be numerically integrated to compute the simulated system's time response;
- the time advances in discrete steps of width h ; the system's evolution is updated at each interval h , rather than continuously.

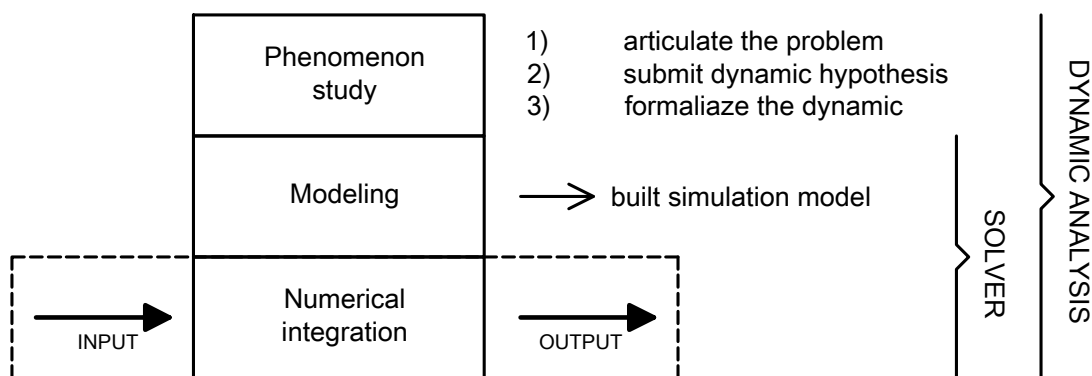


Figure 1.1: Digital simulation.

In practice, the resolution of a dynamic problem is entrusted to a solver. A solver is a piece of mathematical software, possibly in the form of a stand-alone computer program or as a software library, that 'solves' a mathematical problem. A solver

takes problem descriptions in some sort of generic form (e.g. a model) and calculates their solution. The diagram in Figure 1.1 illustrates the the structure necessary for a digital simulation. First, it is necessary to study the phenomenon to be simulated: articulating the problem and making dynamic assumptions form the foundation for formalizing the dynamic problem. Modeling the phenomenon involves creating the simulation model by formulating a set of differential equations that describe the system's dynamic behavior. Finally, through numerical integration of the model, starting from the system's input, the system responses can be calculated.

1.3 Digital simulations challenges

Digital simulations involve several aspects that need to be addressed to obtain acceptable results: from modeling to the numerical implementation of the model. In the two following subsection are presented two main general problems that must be considered in any simulation implementation.

- The definition of the time step (h): it is essential for running any simulation and it depends on the specific application.
- The stiffness of the model: in such cases, numerical integration must be handled in a specific manner to ensure solution convergence.

Other simulation issues such as managing jitter and nonlinearities will be addressed in a subsequent chapter, as they must be addressed more specifically depending on the application.

1.3.1 Time step

The time step (h) is the update rate of the system's evolution; thus, it must be sufficiently small to ensure the convergence of the numerical model and adequate accuracy of the results, but large enough not to significantly impact the required computation power or time, depending on what is prioritized in the application. The simulation step is dictate by the frequency of the highest transient to simulate: according to the rule of thumb it should be smaller than 5% to 10% of the smallest time constant (τ) of the system. To summarize the integration step size must be:

- small enough to capture all the relevant dynamics;
- long enough to limit the calculation time impact on the process itself.

In physics and engineering the time constant (τ) is the parameter characterizing

the response to a step input of a first-order Linear Time Invariant (LTI) system³. Physically, the time constant represents the elapsed time required for the system response to decay to zero if the system had continued to decay at the initial rate, because of the progressive change in the rate of decay the response will have actually decreased in value to $\frac{1}{e} \approx 36.8\%$ in this time (say from a step decrease). In an increasing system, the time constant is the time for the system's step response to reach $1 - \frac{1}{e} \approx 63.2\%$ of its final (asymptotic) value (say from a step increase). In radioactive decay the time constant is related to the decay constant, and it represents both the mean lifetime of a decaying system (such as an atom) before it decays, or the time it takes for all, but 36.8% of the atoms, to decay.

1.3.2 Stiffness

In mathematics, a stiff equation is a differential equation for which certain numerical methods for solving the equation are unstable, unless the step size (h) is taken to be extremely small. It has proven difficult to formulate a precise definition of stiffness, the main idea is that the equation includes some terms that can lead to rapid variation in the solution. These equations present a formidable challenge for ordinary numerical techniques. Regrettably, accurately representing physical systems such as electrical circuits or chemical reactions often are stiff problems.

Considering a linear constant coefficient in-homogeneous system:

$$\dot{\mathbf{x}} = \mathbf{A}\mathbf{x} + f(\mathbf{z}) \tag{1.2}$$

where $\mathbf{x}, \mathbf{z} \in R^M$ and \mathbf{A} is a constant matrix, diagonalizable, $M \times M$ matrix with eigenvalues⁴ $\lambda_m \in \mathbb{C}, m = 1, 2, \dots, M$. Let $\bar{\lambda}$ and $\underline{\lambda}$ be defined by:

$$|Re(\bar{\lambda})| > |Re(\lambda_m)| > |Re(\underline{\lambda})|, m = 1, 2, \dots, M \tag{1.3}$$

We might define the stiffness ratio to quantify the property of the system of differential equations in relative terms, as follows:

$$\frac{|Re(\bar{\lambda})|}{|Re(\underline{\lambda})|} \tag{1.4}$$

Given the challenge of precisely defining stiffness in mathematical terms, here are sentences provided to aid comprehension.

³**Linearity** refers to a system where the outputs resulting from a linear combination of inputs are equivalent to the linear combination of the individual responses to those inputs. **Time invariant** refers to a system where the outputs does not depend on when an input was applied.

⁴A number λ is an eigenvalue of an (M,M) matrix \mathbf{A} if there is a nonzero M vector \mathbf{z} such that $\mathbf{A}\mathbf{z} = \lambda\mathbf{z}$. The corresponding vector \mathbf{z} is said to be an eigenvector of the matrix \mathbf{A} .

- The stiffness arises from the coexistence of very slow and very fast dynamics.
- Stiffness occurs when some components of the solution decay much more rapidly than others.
- A linear constant coefficient system is stiff if all of its eigenvalues have negative real part and the stiffness ratio is large.
- Stiffness occurs when stability requirements, rather than those of accuracy, constrain the step length.
- If a numerical method with a finite region of absolute stability⁵, applied to a system with any initial conditions, is forced to use in a certain interval of integration a step length which is excessively small in relation to the smoothness of the exact solution in that interval, then the system is said to be stiff in that interval.

1.4 Electrical dynamic systems

Simulation tools are at the base for the design and test of systems in all the engineering sectors. In electrical engineering are used extensively for all the aspects concerned the power systems (from the very large high-voltage transmission systems to the very low power drivers) and for various applications (from the long-term planning to transient analysis). Furthermore, in the next years the simulation contributions will be fundamental to adapt the global electric network to two main topics: the advent of the electrification era and the climate change. The first will implicate a massive integration in the network of completely new features, in a system not designed to support them, such as multi levels parkings equipped with charging stations for electrical vehicles or large size photovoltaic plants. Moreover, the intensification of extreme weather events, related to the climate change, are making central the theme of network resilience. The complexity of the challenge is in the high grade of interconnection of the electrical infrastructures: a single event may have an impact on a large area. Therefore new equipment and strategies should be tested and validated on virtual environment before the implementation, in order to evaluate their impact on the whole system, not predictable in advance.

The time constants (τ) involved vary depending on the electrical system and the type of analysis that needs to be conducted. Figure 1.2 illustrates the the time scales in function of the electrical transients to be studied. The dissertation focuses

⁵The stability region, defined in the complex plane, comprises points where the condition $z \in \mathbb{C} | \phi(z) < 1$ holds true, with $\phi(z)$ stability function of the method.

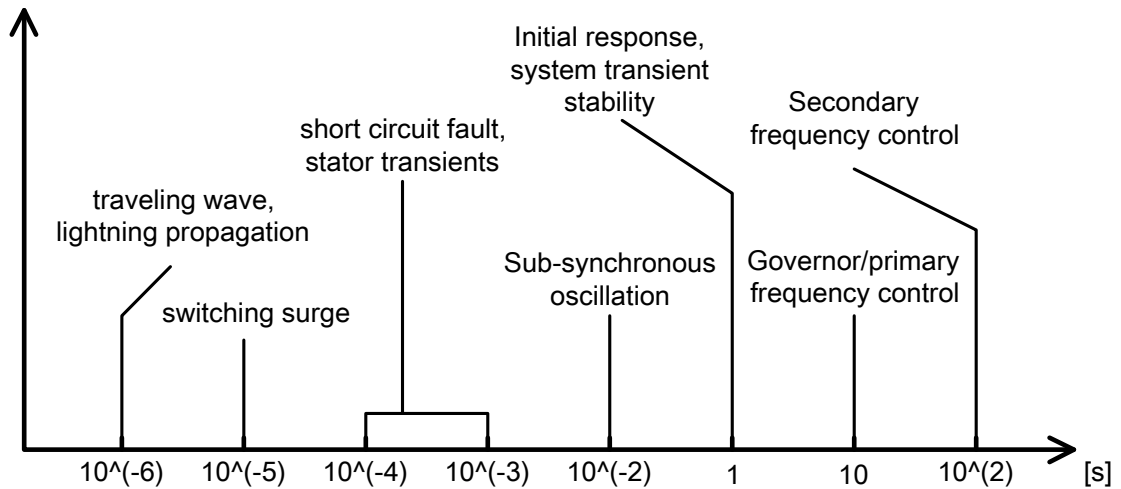


Figure 1.2: Simulation time scales in power system.

on Electromagnetic Transient (EMT) of power systems, so the primary transients of interest and, consequently, the elements to be modeled are:

- synchronous machine;
- excitation system;
- steam turbine and governor;
- load modeling;
- transmission line modelling.

The complexity of the simulation, in terms of computational burden, depends on the required simulation speed and the size of the network to be analyzed. This is primarily determined by the number of connected generators, as they are the main dynamic elements of the electrical system (see Figure 1.3).

An unmanned aerial vehicle (UAV), commonly known as a drone, is an aircraft without any human pilot, crew, or passengers on board.

A Flexible AC Transmission Systems (FACTS) is a family of Power-Electronic based devices designed for use on an Alternating Current (AC) Transmission System to improve and control Power Flow and support Voltage. FACTS devices are alternatives to traditional electric grid solutions and improvements, where building additional Transmission Lines or Substation is not economically or logistically viable.

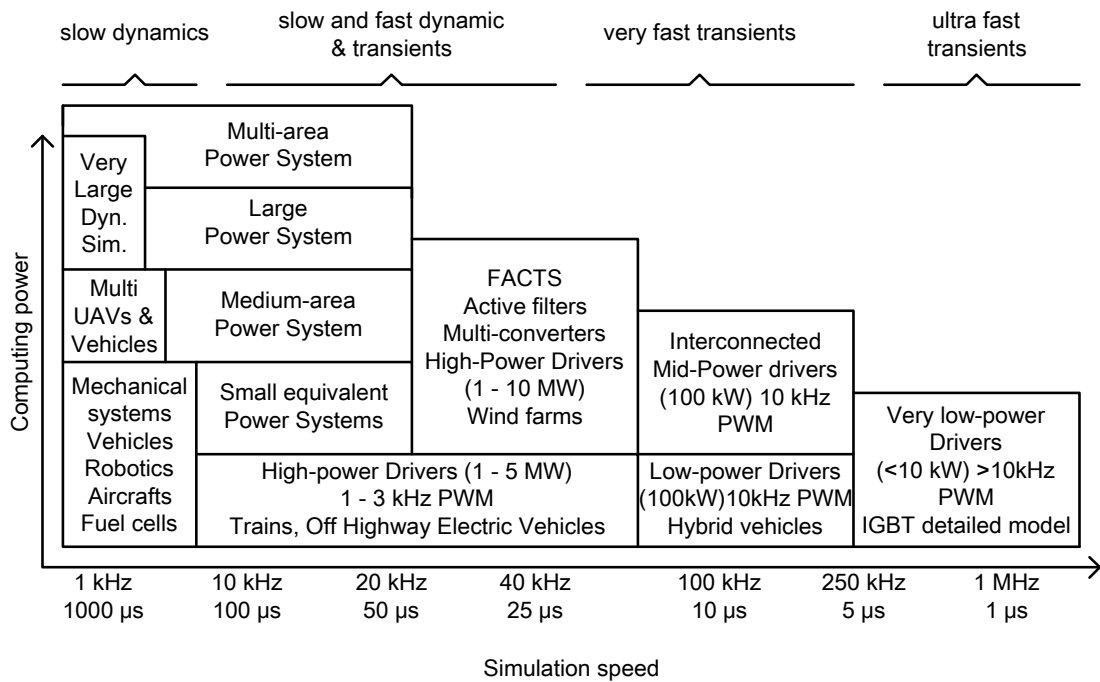


Figure 1.3: Simulation time step by application.

Chapter 2

Mathematical tools

This chapter briefly presents the main mathematical tools that form the foundation of the entire dissertation. It is important to understand the mathematical operations performed by these tools in order to:

- select the best one when multiple options are available for the same task;
- have a clear understanding of the output derived from the model. It is essential to critically evaluate the results when modeling phenomena, as simulation artifacts often arise from the integration method used rather than from the model itself.

2.1 Numerical Integration

In analysis, numerical integration comprises a broad family of algorithms for calculating the numerical value of a definite integral. The basic problem in numerical integration is to compute an approximate solution to a definite integral $\int_a^b f(x) dx$ to a given degree of accuracy (see Figure 2.1). If $f(x)$ is a smooth function integrated over a small number of dimensions, and the domain of integration is bounded, there are many methods for approximating the integral to the desired precision. The main themes related to the numerical integration of models are:

- the stability property, which is a feature of algorithms that can be proven to avoid magnifying approximation errors;
- robustness, which pertains to algorithms that do not produce significantly different results when there are very small changes in the input data;
- the accuracy, which is the ability to produce results close to the true value.

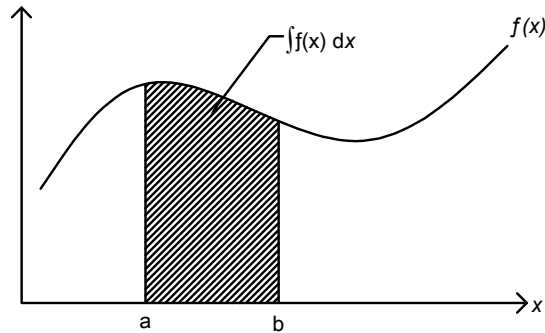


Figure 2.1: Numerical integration.

Since numerical integration is fundamental to digital simulation (see Paragraph 1.2), this section provides a more detailed discussion on the topic. Starting from a brief introduction on the categorisation of methods. For a deep understanding of the math behind what is presented in this chapter use references [1] and [2].

Let's begin with a brief overview of how methods can be categorized. Numerical methods can be, first of all, classified in explicit and implicit methods. Explicit methods directly calculate the state of a system¹ ($x(t)$) at the later time $t_c + h$ from the state of the system at time t_c as in equation 2.1:

$$x(t_c + h) = f(x(t_c), u(t_c), h) \quad (2.1)$$

In implicit methods, the calculation of the state of a system ($x(t)$) at the later time $t_c + h$ depends from the state of the system at the same time as in equation 2.2:

$$x(t_c + h) = f(x(t_c), x(t_c + h), u(t_c), h) \quad (2.2)$$

Whit $x(t)$ the state of the system, $u(t)$ the input of the system and h the time step. The main drawback of implicit methods is the additional computational cost that derives from the required simultaneous solution of all the equations of the considered system; this may require at least one matrix inversion per simulation step (assuming a generic non-linear system). Explicit methods vice versa have, typically, a smaller computational cost but, at the same time, they require, usually, a smaller time step to be stable and accurate.

Another important classification for integration methods has to be done between single- and multi-step methods. Single-step methods are based on the previous

¹The state of a system at any time instant t_c is the minimal amount of information that, together with all inputs for $t > t_c$, uniquely determines the behavior of the system for all $t > t_c$. The concept will be explored in more detail in the next chapter.

solution of the state and, depending on the specific method used, they may require multiple derivative evaluations. Multi-step methods, with the purpose of limiting the number of derivatives evaluations, use multiple previous steps. Single-step methods are more diffused as a consequence of their simplicity of implementation, nevertheless, multi-step methods have to be in general considered as a valid alternative due to the significant computational cost reduction they may offer.

2.1.1 Stiff solvers

Most engineering models result in systems of stiff equations, which encounter stability issues during numerical resolution (see subsection 1.3.2). To simulate these systems with a non-stiff solver, you will be forced to adapt the time step to higher frequency component of the particular dynamic and the simulation will become extremely expensive for the frequency of interest. However, a specific class of solvers, known as "stiff solvers", are able to “cut through” the high-frequency components and be less influenced by frequency components higher than sampling frequency. These methods, characterized as A-stable and L-stable, excel in this regard.

The A-stability is demonstrated applying the test equation $\dot{x} = kx$ with $x(0) = 1$ and $k \in \mathbb{C}$. The solution of the equation is $x = e^{kt}$. This solution approach zero as $t \rightarrow \inf$ when $Re(k) < 0$. If the numerical method also exhibits this behaviour (for a fixed step size), then the method is said to be A-stable. Another possible definition is by the stability region²: the method is A-stable if the region of absolute stability contains the set $z \in \mathbb{C} | Re(z) < 0$, that is the left half complex plane (figure 2.2). L-stability is a special case of A-stability: a method is L-stable if it is A-stable and $\overline{\Phi(z)} \rightarrow 0$ as $z \rightarrow 0$, where $\Phi(z)$ is the stability function of the method³. A numerical method that is L-stable has the stronger property that the solution approaches zero in a single step as the step size goes to infinity.

2.1.2 Euler forward method

The Euler methods are simple methods of solving first-order ODE, particularly suitable for quick programming because of their great simplicity. Let us consider the system in equation 1.1 and let us assume that t_c is the current time and $x(t_c)$ is the value of current state, our goal is to calculate the value of the future state

²The stability region, defined in the complex plane, comprises points where the condition $z \in \mathbb{C} | \phi(z) < 1$ holds true, with $\phi(z)$ stability function of the method.

³The stability function of the numerical method is the solution obtained from the application of the test equation $\dot{x} = kx$ into the complex plane.

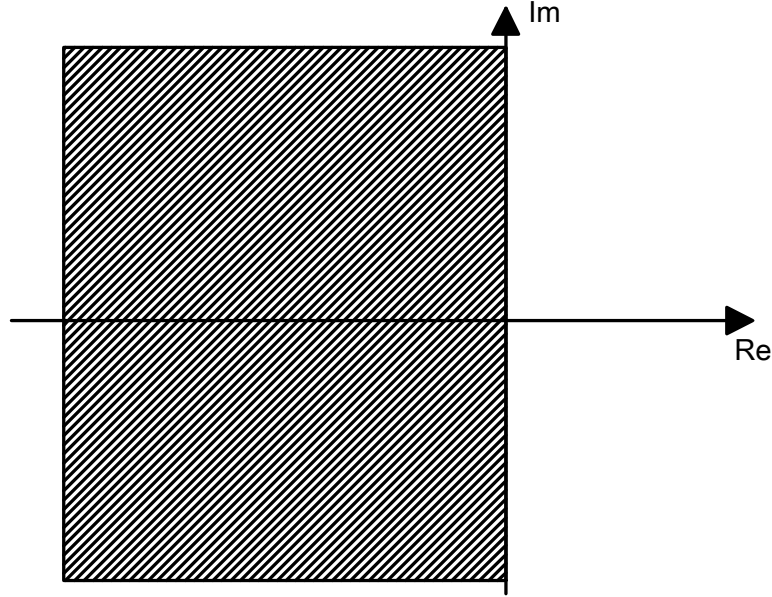


Figure 2.2: Stability region of trapezoidal method (A-stable).

$x(t_c + h)$. For a small enough h , the derivatives of $x(t_c)$ at t_c can be approximated by the forward difference as in equation (2.3):

$$\dot{\mathbf{x}}(t_c) \approx \frac{\mathbf{x}(t_c + h) - \mathbf{x}(t_c)}{h} \quad (2.3)$$

This implies:

$$\mathbf{x}(t_c + h) \approx \mathbf{x}(t_c) + h\dot{\mathbf{x}}(t_c) \quad (2.4)$$

By ignoring the approximation, we get:

$$\mathbf{x}(t_c + h) = \mathbf{x}(t_c) + h \cdot f(t_c, \mathbf{x}(t_c), \mathbf{u}(t)) \quad (2.5)$$

Looking at equation 2.5, it is clear that the obtained method is explicit. This method is usually referred as the Euler forward method.

Let us now consider the linear-time invariant differential equation 2.6:

$$\dot{\mathbf{x}} = \lambda \mathbf{x} \quad (2.6)$$

Applying the Euler forward integration method, we obtain:

$$\mathbf{x}(t_c + h) = (1 + \lambda h)x(t_c) \quad (2.7)$$

As a consequence, the integration is stable only if:

$$|1 + h\lambda| \leq 1 \quad (2.8)$$

From equation 2.8, the stability domain of the Euler forward method can be drawn in the complex plane $h\lambda$ (Figure 2.3).

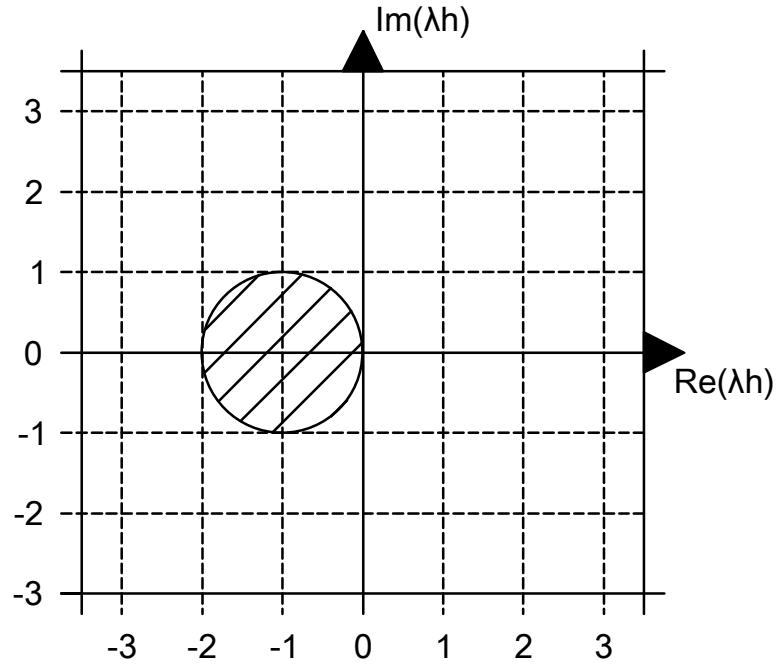


Figure 2.3: Stability region of the Euler Forward integration method.

2.1.3 Euler backward method

Let us now still consider the system in equation 1.1 but let us approximate the derivatives of $x(t)$ at t_c by the backward difference as in equation 2.9:

$$\dot{\mathbf{x}}(t_c + h) \approx \frac{\mathbf{x}(t_c + h) - \mathbf{x}(t_c)}{h} \quad (2.9)$$

Rearranging the terms, we get:

$$\mathbf{x}(t_c + h) \approx \mathbf{x}(t_c) + h \cdot \dot{\mathbf{x}}(t_c + h) \quad (2.10)$$

By ignoring the approximation:

$$\mathbf{x}(t_c + h) = \mathbf{x}(t_c) + h \cdot f(t_c + h, \mathbf{x}(t_c + h), \mathbf{u}(t_c + h)) \quad (2.11)$$

The integration method obtained in equation 2.11 is known as the backward Euler method and, as it can be seen, is an implicit method. Applying Euler backward integration method to the equation in 2.6, equation 2.12 is obtained.

$$\mathbf{x}(t_c + h) = \left(\frac{1}{1 - h\lambda} \right) \mathbf{x}(t_c) \quad (2.12)$$

As a consequence, the integration using the Euler backward method will be stable only if:

$$\left| \frac{1}{1 - h\lambda} \right| \leq 1 \quad (2.13)$$

From equation 2.13, the stability domain of the Euler backward method can be drawn in the complex plane $h\lambda$ (Figure 2.4).

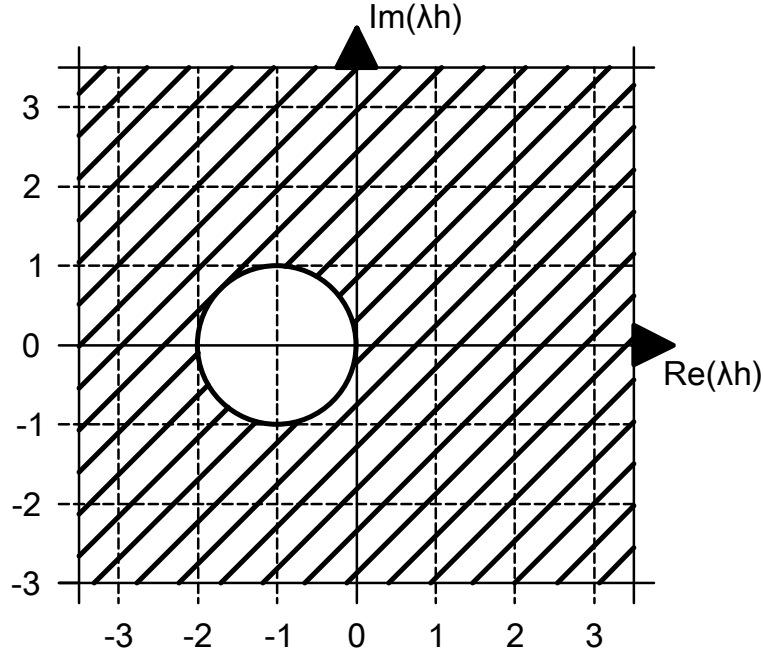


Figure 2.4: Stability region of the Euler Backward integration method.

2.1.4 Trapezoidal rule method

Let us now consider a different integration method largely known with the name of trapezoidal rule. In this case, the calculation of the area between the curves we want to integrate and the $y = 0$ axis is linearly approximated. Equation 2.14 presents the integration scheme for the trapezoidal rule.

$$\mathbf{x}(t_c + h) = \mathbf{x}(t_c) + \frac{h}{2}(f(t_c + h, \mathbf{x}(t_c + h), \mathbf{u}(t_c + h)) + f(t_c, \mathbf{x}(t_c), \mathbf{u}(t_c))) \quad (2.14)$$

The trapezoidal rule integration method is a second-order single-step method, it is a very well-known implicit method that presents two extremely interesting properties that made its fortune.

- It is stable, compared with Euler backward method.
- It does not present the inconvenient of making unstable system in nature stable in simulation like Euler backward method: its stability domain is limited to the left half of the complex plane λh

Applying the trapezoidal rule to the equation in 1.1, (2.17) is obtained.

$$\mathbf{x}(t_c + h) = \mathbf{x}(t_c) + \frac{h}{2}\lambda\mathbf{x}(t_c) + \frac{h}{2}\lambda\mathbf{x}(t_c + h) \quad (2.15)$$

Regrouping the terms, we get:

$$\mathbf{x}(t_c + h) = \frac{1 + \lambda\frac{h}{2}}{1 - \lambda\frac{h}{2}}\mathbf{x}(t_c) \quad (2.16)$$

The trapezoid rule method is stable if:

$$\left| \frac{1 + \lambda\frac{h}{2}}{1 - \lambda\frac{h}{2}} \right| \leq 1 \quad (2.17)$$

As anticipated before, the stability domain of trapezoidal rule includes all and only the left half plane of λh .

2.1.5 Higher order methods

The Euler forward method is often inefficient due to the small step size needed to achieve a specified accuracy. Additionally, round-off error accumulation over many steps can render the numerical results unusable. To improve the accuracy of the obtained solutions, higher-order methods are available. In this chapter, these methods are mentioned solely to provide a comprehensive overview of integration methods, as they are not essential for the analysis. For a more detailed study, refer to [1] and [2].

- Predictor and corrector methods. The predictor and corrector integration method is based on two evaluations of the derivative. The predictor, using an explicit method, calculates a rough estimation of the value for the next step of the function to be integrated. The corrector, using an implicit method, calculates the final value for the next step of the function to be integrated on the base of the value computed by the predictor. The scheme has to be classified as an explicit method.
- Runge-Kutta methods. The first-order Runge–Kutta method, often abbreviated in RK1, is equivalent to Euler forward (section 2.1.2). The second-order Runge–Kutta method, RK2, also known as explicit midpoint rule, can be interpreted as a two-stage predictor and corrector. By further increasing the integrative order, the RK3 and RK4 methods are identified.

- Adams-Bashforth and Adams-Moulton methods. Compared to Runge-Kutta methods, Adams–Bashforth methods are less computationally costly, since only one function evaluation is required, probably a much smaller time step will be required. As a consequence, the selection of a Adams–Bashforth integration method instead of a Runge–Kutta one should be done after accurate evaluation of the system to be integrated. Instead, the Adams–Moulton methods are a simple example of the implicit multi-step method. To note that Adams–Bashforth and Adams–Moulton methods can be combined together to define very stable predictor and corrector schemes.

2.1.6 Accuracy comparison

The accuracy comparison of the various presented methods is illustrated in Figure 2.5. The frequency response obtained with the discrete time transfer function⁴ with the one obtained by the continuous time transfer function are correlated. As a reference case it is taken into account the characteristic equation of an inductor. This analysis is sourced from the reference book [3].

$$H(z) = \frac{I(z)}{V(z)} \quad (2.18)$$

An interesting aspect to notice is that the trapezoidal rule not only has a really convenient region of stability, as it has already been shown, but it is also extremely accurate if compared to other integration methods of similar order.

2.2 Lower-Upper (LU) factorization

In numerical analysis and linear algebra, the LU decomposition or factorization is one of the most commonly used methods for solving linear systems. It factors a matrix into the product of a lower triangular matrix and an upper triangular matrix, providing a straightforward approach to solving linear equations.

$$\mathbf{Y}\mathbf{v} = \mathbf{b} \rightarrow \mathbf{L}\mathbf{U}\mathbf{v} = \mathbf{b} \rightarrow \mathbf{L}\mathbf{z} = \mathbf{b} \rightarrow \mathbf{U}\mathbf{v} = \mathbf{z} \quad (2.19)$$

In both cases we are dealing with triangular matrices (\mathbf{L} and \mathbf{U}), which can be solved directly by forward and backward substitution without using the Gaussian

⁴In the frequency domain analysis of systems the term "transfer function" is the amplitude of the output as a function of the frequency of the input signal. The transfer function of an electronic filter is the amplitude at the output as a function of the frequency of a constant amplitude sine wave applied to the input.

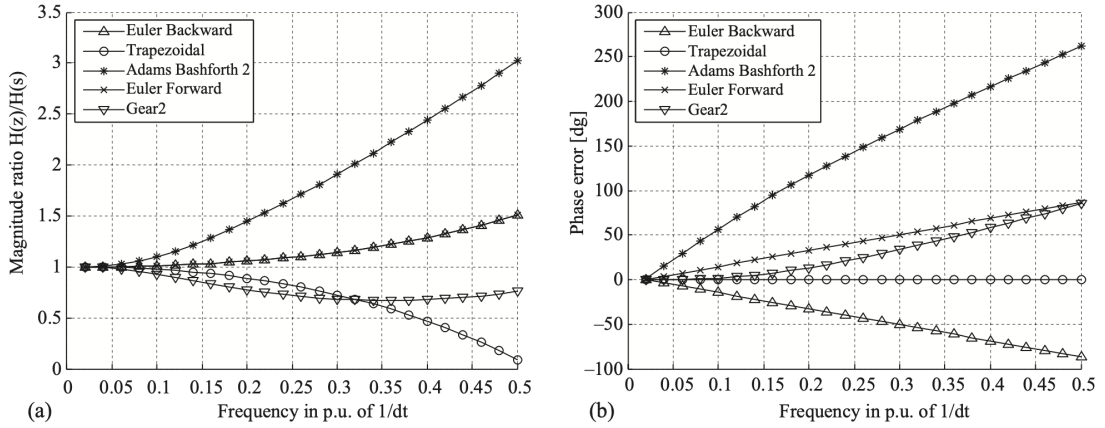


Figure 2.5: Accuracy comparison: (a) magnitude and (b) phase (sourced from the reference [3]).

elimination process⁵ (however we do need this process or equivalent to compute the LU decomposition itself). It is faster (and more convenient) to do an LU decomposition of the matrix \mathbf{Y} once and then solve the triangular matrices for the different \mathbf{b} , rather than using Gaussian elimination each time. The matrices L and U could be thought to have "encoded" the Gaussian elimination process.

The cost of solving a system of linear equations is approximately $\frac{2}{3}M^3$ floating-point operations if the matrix \mathbf{Y} has size M .

⁵In mathematics, Gaussian elimination, also known as row reduction, is an algorithm for solving systems of linear equations. It consists of a sequence of row-wise operations performed on the corresponding matrix of coefficients, in order to modify the matrix until the lower left-hand corner of the matrix is filled with zeros, as much as possible.

Chapter 3

Electrical systems modeling

The modeling of electrical systems is grounded in two distinct approaches detailed in the following sections:

- the nodal method;
- the State Space (SS) technique.

3.1 Nodal approach

The nodal method, also known as the topological approach, represents electrical systems using a series of algebraic equations. Its fundamental principle is to formulate an algebraic equation for each node within the network under examination, with the node's voltage as the unknown variable, utilizing the foundational laws of electrotechnics.

In a DC network composed by B branches and N nodes there are $2B$ unknowns: the voltage and the current in each branch. It can be shown that the problem is well-structured and it can be solved since it is possible to write a system of $2B$ independent equations. From the circuit theory the available equations are:

- Kirchhoff's Current Law (KCL) \rightarrow Kirchhoff's current laws;
- Kirchhoff's Voltage Law (KVL) \rightarrow Kirchhoff's voltage laws;
- characteristic equations (Ohm's law in a broad sense).

It is easy to see that each branch is described by a characteristic equation and it could be demonstrated that only $N - 1$ KCL and $B - N + 1$ KVL are independent [3].

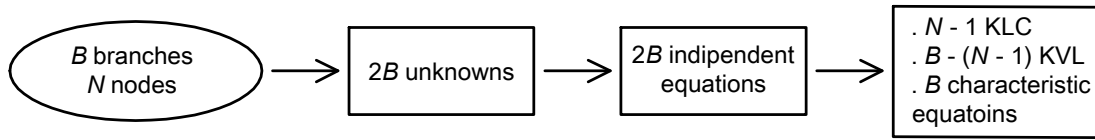


Figure 3.1: Algebraic system formation

Through the application of the nodal principle the system size is reduced from $2B$ to $N - 1$, significantly reducing the number of equations that must be solved simultaneously at each time step. This principle can be summarized in the following three steps:

1. $N - 1$ independent voltages are chosen (for example the voltages at each node with reference to a node selected as a reference);
2. by the application of the KVL the branch voltages are related to the node potentials;
3. by the application of the generalised Ohm's law the currents in each written KCL are removed.

The resultant is a system of $N - 1$ nodal equations with node potentials as variables. It is convenient to write the set of equations in matrix form (eq. 3.1) in order to exploit numerical methods, such as the most common LU factorisation (see section 2.2), to obtain directly the vector of nodal potential \mathbf{v} . Computationally speaking, the solution of the linear problem is a very intense problem with a complexity that is approximately proportional to the third power of the size of the system. As results of this, the reduction of the number of unknowns has a very significant impact on the complexity of the problem. The reduction in system size allows for a decrease in computation time and required memory. It is worth noting that the admittance matrix (\mathbf{Y}) remains unchanged if the network topology remains constant and the time-step (h) is constant. This is why the solver must operate with a fixed calculation step: with the constant \mathbf{Y} matrix it is possible to compute its LU factorization only once offline and then solve the triangular matrices for the different \mathbf{b} , without using the Gaussian elimination process, saving additional computation time. Furthermore, the algorithm leverages the sparsity property of the matrix and implements ordered elimination schemes to minimize the usable calculation step.

$$\mathbf{Y}\mathbf{v} = \mathbf{b} \quad (3.1)$$

Whit:

- \mathbf{Y} \rightarrow admittance matrix

- \mathbf{v} \rightarrow vector of nodal potentials
- \mathbf{b} \rightarrow input's vector

In general, when modeling, the modified nodal principle is applied. This method involves introducing one additional equation and unknown (the current through the source) [3] to also represent ideal voltage generators, which are crucial for modeling real devices such as controlled power supplies.

The nodal approach is very simple to apply with a Direct Current (DC) network. Each foundational element within the network may be expressed by the specific equation 3.2. Then the system of nodal equations (eq. 3.1) can be automatically constructed simply by examining the system's topology and appropriately aggregating, through superposition of effects¹, the matrix models of the various basic components (ideal voltage generators, ideal current generators and resistors). The "matrix stamps" of the base DC components are reported in the table 3.1.

$$\mathbf{Y}_p \mathbf{v} = \mathbf{b}_p \tag{3.2}$$

In order to analyse Alternate Current (AC) networks is necessary to introduce the resistive companion principle. The solution of transient equation is based on the transformation of every dynamic element in an equivalent DC circuit representing an iteration of an integration method (see section 2). The lumped parameters are modelled by integrating their corresponding differential equations. For the branches with distributed parameters an exact solution can be obtained with the method of characteristics by neglecting their losses in order to have integrable differential equation from the D'Alembert dissertation². Refer to table 3.2. The branch's lossess could be modelled as lumped resistance at both ends of the line.

When dealing with a multiphase network, it becomes imperative to account for the mutual coupling between phases. In practical applications, the scalar quantities of a single branch are replaced by matrix quantities for the set of branches, where the off-diagonal elements are determined by the mutual coupling. However, the modeling described earlier remains unchanged.

¹The superposition principle, also known as superposition property, states that, for all linear systems, the net response caused by two or more stimuli is the sum of the responses that would have been caused by each stimulus individually. So that if input b_1 produces response y_1 , and input b_2 produces response y_2 , then input $b_1 + b_2$ produces response $(y_1 + y_2)$.

²D'Alembert presents a general resolution to the differential equation governing tension and current along the line ($-\frac{\partial e}{\partial d} = \dot{L} \frac{\partial i}{\partial t}$ and $-\frac{\partial i}{\partial d} = \dot{C} \frac{\partial e}{\partial t}$), rewritten them in two wave equations algebraically expressed as: $i(d, t) = f_1(d-wt) + f_2(d+wt)$ and $e(d, t) = Z f_1(d-wt) - Z f_2(d+wt)$.


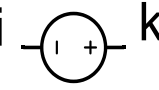
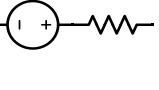
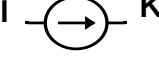
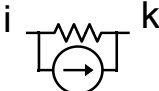
BASE ELEMENT	SYMBOL	\mathbf{Y}_p	\mathbf{b}_p
Resistors		$\begin{bmatrix} 1/R & -1/R \\ -1/R & 1/R \end{bmatrix}$	-
Ideal voltage generator		$\begin{bmatrix} & 1 \\ 1 & -1 \end{bmatrix}$	$\begin{bmatrix} \\ V \end{bmatrix}$
Real voltage generator		$\begin{bmatrix} 1/R & -1/R \\ -1/R & 1/R \end{bmatrix}$	$\begin{bmatrix} -V/R \\ V/R \end{bmatrix}$
Ideal current generator		-	$\begin{bmatrix} -I \\ I \end{bmatrix}$
Real current generator		$\begin{bmatrix} 1/R & -1/R \\ -1/R & 1/R \end{bmatrix}$	$\begin{bmatrix} -I \\ I \end{bmatrix}$

Table 3.1: Matrix stamps of the basic DC components.

3.2 State Space (SS) approach

Another very common and widely used family of EMT modeling approaches is the one based on state-space representation. Compared to the nodal method, it can be observed that the number of variable to be calculated at each iteration is minor: reducing the number of variable calculated at each time step reduce the simulation execution time. On the other hand, the computer implementation of models is more complicated: it often requires the direct involvement of a user with a significant experience in modeling, it is extremely error prone and it may lead to the creation of simulation artifacts hard to identify.

The state of a dynamic system contains all the information needed to calculate responses to present and future inputs without reference to the past history of its inputs and outputs. The state of a system at any time instant t_c is the minimal amount of information that, together with all inputs for $t > t_c$, uniquely determines the behavior of the system for all $t > t_c$. Typically, in an electrical system, the number of state variables is determined by the number of independent energy

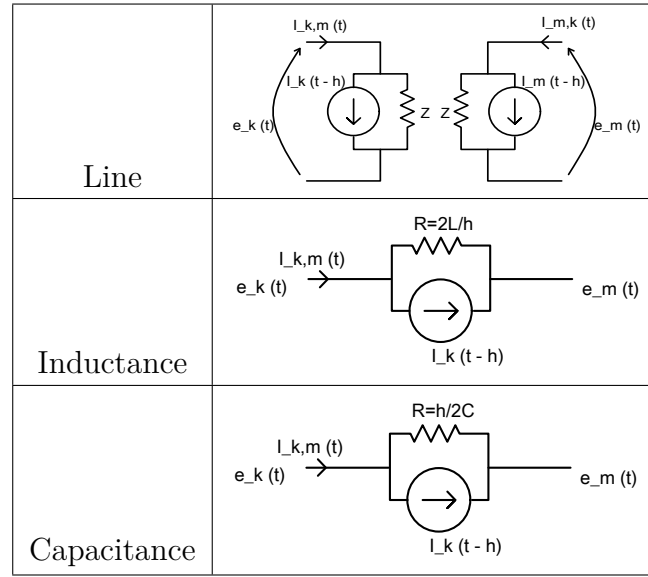


Table 3.2: Resistive companion modeling of dynamic components.

storage elements and it includes the current flowing through inductors and the voltage across capacitors.

The mathematical description of a system based on state-space modeling is obtained by a set of n coupled first-order ordinary differential equations known as the state equations, in which the time derivative of each state variable $\dot{x}_i(t)$ is expressed in terms of the state variables $x_1(t); x_2(t); \dots; x_J(t)$ and of the inputs $u_1(t); u_2(t); \dots; u_K(t)$ of the system. Where 'J' the number of state variables and 'K' the number of inputs variables. In general:

$$\dot{\mathbf{x}}(t) = \mathbf{f}(\mathbf{x}(t), \mathbf{u}(t), t) \quad (3.3)$$

Assuming an LTI system³ we can express the relation between each state variable derivative $\dot{x}_i(t)$ as the weighted sum of the state variables and the system inputs (eq. 3.4). Additionally, it's convenient to characterize the physical system in terms of P output variables, $\mathbf{y}(t)$, which are of engineering interest and may not align with the state variables (eq. 3.5).

$$\dot{\mathbf{x}}(t) = \mathbf{A}\mathbf{x}(t) + \mathbf{B}\mathbf{u}(t) \quad (3.4)$$

$$\mathbf{y}(t) = \mathbf{C}\mathbf{x}(t) + \mathbf{D}\mathbf{u}(t) \quad (3.5)$$

³**Linearity** refers to a system where the outputs resulting from a linear combination of inputs are equivalent to the linear combination of the individual responses to those inputs. **Time invariant** refers to a system where the outputs does not depend on when an input was applied.

Whit:

- $\mathbf{A} \in \mathbb{R}^{J,J}$ the system matrix
- $\mathbf{B} \in \mathbb{R}^{J,K}$ the input matrix
- $\mathbf{C} \in \mathbb{R}^{P,J}$ the output matrix
- $\mathbf{D} \in \mathbb{R}^{P,K}$ the feed forward matrix

As previously mentioned, the complexity of the method lies in circuit modeling, which is not always straightforward. Hence, it is worth noting an approach, here not explored, outlined in [4] for automatically generating state-space models by assuming a specific structure for individual components.

Once the continuous-time state-space model is built it needs to be converted into a discrete-time state-space model through an integration process (see section 2.1) to enable computer simulation. The system resulting from the discretization is presented in eq. 3.6 and eq. 3.7. It should be observed that the time instant to which the input vector refers is determined by the specific integration method applied.

$$\mathbf{x}(t_c + h) = \mathbf{A}_{disc}\mathbf{x}(t_c) + \mathbf{B}_{disc}\mathbf{u}(t_c + h) \quad (3.6)$$

$$\mathbf{y}(t_c + h) = \mathbf{C}_{disc}\mathbf{x}(t_c + h) + \mathbf{D}_{disc}\mathbf{u}(t_c + h) \quad (3.7)$$

In any case, the most common way to simulate a system modeled using a state-space representation is not to directly integrate a system representation in the form of (eq. 3.4 and eq. 3.5) but to use what is normally referred as a signal solver. In a signal solver, the system modeled using state-space representation is represented by a block diagram, the solution is computed by solving each block independently. For each block, the output is computed starting from its inputs values obtained from the solution at the previous time step. It is clear that this solution process implies the use of an explicit integration method.

Chapter 4

Real Time Simulation (RTS)

Real Time Simulation (RTS) is a critical tool for modern engineering and system design, providing a versatile and dynamic means to analyze, test, and validate complex systems. Its ability to deliver immediate feedback and facilitate interactive engagement makes it indispensable in industries where precision and responsiveness are paramount. As technology continues to advance, the capabilities and applications of real-time simulation are poised to expand even further, driving innovation and efficiency across a broad spectrum of disciplines.

Real Time Simulation (RTS) is a powerful technique used across various fields, including engineering, computer science, and systems design, to model and analyze the behavior of complex systems in a dynamic environment. Unlike traditional simulations, which may run slower than or independent of real time, real-time simulations are designed to operate at the same pace as the actual processes they mimic. This allows for immediate feedback, interaction, and control, making them invaluable in applications where timely responses are critical. The simulations presented in figure 4.1 a) and b) obtain the solution of the model, respectively, in advance and late respect to the simulation clock. In any case they proceed to the solution of the next time step. This is characteristic for offline simulations since they aim to obtain the results as fast as possible. The system solving speed depends on available computation power and the system's mathematical model complexity. In real-time simulation, the computer model runs at the same rate as the actual physical system, see case c) in figure 4.1. The time required to compute the solution at a given time-step must be shorter than the wall clock duration of the time step. Any idle time of the fixed-time step is lost, the simulator wait until the clock tick to the next time step. If simulator operations are not all achieved within the required fixed time-step, the real-time simulation is considered erroneous

(overrun error). It is clear that the accuracy of computations not only depends on precise dynamic representation of the system, but also on the length of time used to produce results. Proper time-step duration must be determined to accurately represent system frequency response up to the fastest transient of interest ensuring to achieve real-time without overrun [5].

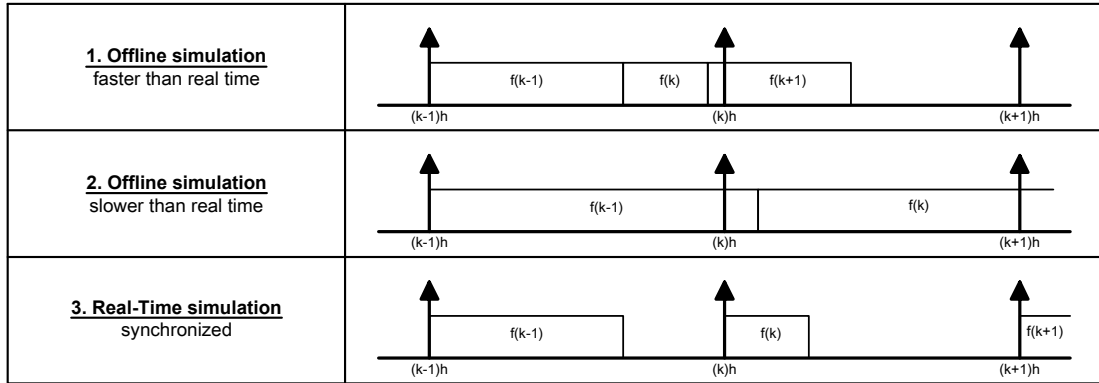


Figure 4.1: Real time simulation requisites and other simulation techniques

The following are key features of this type of simulations.

- **Synchronization with Real-Time Clocks:** the simulation must advance at the same rate as real-world time, ensuring that events and processes occur in synchrony with their actual counterparts.
- **Low Latency and High Throughput:** real-time systems must process data and execute instructions with minimal delay to maintain the fidelity of the simulation and provide accurate, timely outputs.
- **Interactivity:** users can interact with the simulation in real time, allowing for on-the-fly adjustments and immediate observation of results. This is particularly beneficial in training scenarios, where operators can practice responses to various conditions in a safe, controlled environment.
- **Determinism:** the behavior of the simulation must be predictable and repeatable, providing consistent results under the same conditions. This is essential for validating the performance and reliability of control systems.

4.1 Applications

Two primary application categories are identifiable: Software in the Loop (SIL) and Hardware in the Loop (HIL). In SIL configuration, the entire system operates

within a simulator, ensuring signal integrity as no inputs or outputs are utilized. Furthermore, timing synchronization with the external environment becomes non-critical. Simulation speeds faster than real-time can be employed, facilitating a multitude of tests within a brief timeframe. Hence, SIL is ideal for statistical testing, such as Monte Carlo simulations¹. Offline simulations are also valuable when the computational power available isn't adequate for achieving real-time performance. In such cases, the simulation proceeds without encountering overrun errors. On the other side HIL simulations are more interest as technical tool. Virtual plants usually are more constant and cost less than real plants. This allows for more repeatable results and provides for testing conditions that are unavailable on real hardware, such as extreme events testing. Furthermore, when a user or physical equipment interacts with a real-time model, they can provide model inputs and get model outputs, as it would with a real plant. A model executed on a real-time simulator can also be modified online, which is not possible with a real plant. In addition, any model parameter can be read and updated continuously. Figure 4.2 illustrates the advantages of model interaction.

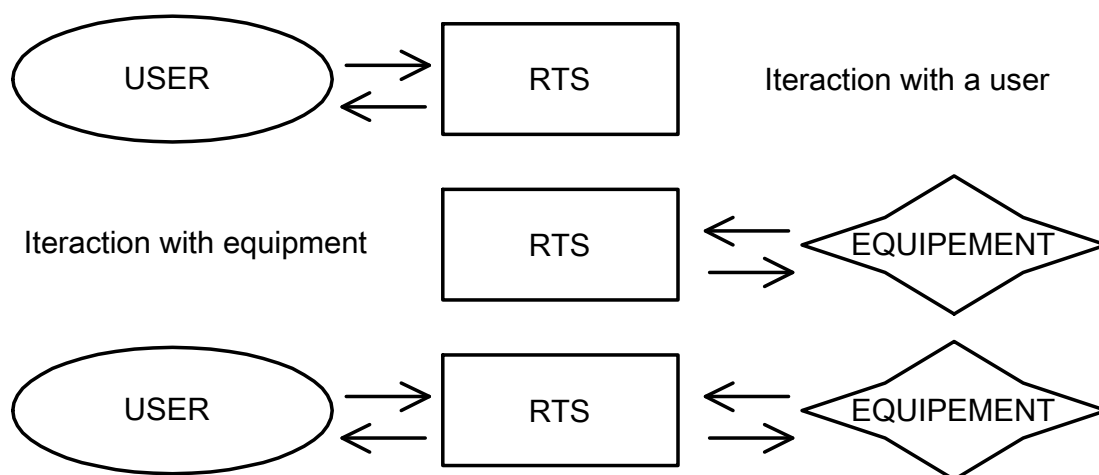


Figure 4.2: Types of simulation interaction.

¹Monte Carlo methods, or Monte Carlo experiments, are a broad class of computational algorithms that rely on repeated random sampling to obtain numerical results. The underlying concept is to use randomness to solve problems that might be deterministic in principle. Monte Carlo methods are mainly used in three distinct problem classes: optimization, numerical integration, and generating draws from a probability distribution. They can also be used to model phenomena with significant uncertainty in inputs.

Model Based Design (MBD)² represents one application of HIL configuration. Employing this approach allows for the early detection of design issues, thereby reducing the duration of the development cycle. Moreover, testing and validation costs can be reduced in to the medium to long term, and the entire system can be tested under conditions that would be costly and dangerous to replicate on a physical prototype or in a real power system. Additionally, automated repetitive testing facilitates the production of statistical data. Such simulations are also highly beneficial for educational purposes and technician training. By incorporating user interfaces, experts can experiment with operations in a safe environment.

The areas of interest span a wide range: power generation applications, automotive applications, electric ships and railway networks, aerospace, electric drive and motor development and testing, and more.

4.2 Hardware setting

Although, physical simulators have served their roles in power systems industry very well; still, they are inconvenient to use as they have the difficulty of immobility and high cost of maintenance. In addition, these physical simulators are required to power up all the network and system setup concurrently. Nonetheless, with the progress of microprocessor and floating-point Digital Signal Processing (DSP) technologies, physical simulators are being gradually replaced with fully digital real-time simulators.

Digital real-time simulators take full advantages of open and modern high-performance distributed parallel supercomputer technologies (PC clusters) used by several scientific application super computer centers. Most commercially available simulators are based on Commercial off-the-shelf (COST) non-proprietary PC modules. As an integrated software and hardware system based on Intel or AMD processors, it combines FPGA-based models to obtain simulation time steps in the order of a few hundred nanoseconds. Moreover, a large number of FPGA-based inputs and outputs (I/O) cards enable high-speed low-latency direct connection with external equipment for hard real-time simulation.

The configuration of the simulator (Figure 4.3) is described as follows.

- There could be more than one target PCs in the overall system; the master PC

²The model-based design is significantly different from traditional design methodology. Rather than using complex structures and extensive software code, designers can use Model-based design to define plant models with advanced functional characteristics using continuous-time and discrete-time building blocks.

executes all the communications with both the target and the host along with all additional target PCs. They are the cores that carry out the simulation.

- Like target PCs, there also could be more than one host PC. Each PC host gives the access to several end-users to ping the targets; where, the master host has the complete control of that simulator. While other hosts are kept in read-only mode which can only receive and show signals from the simulator. I/Os can be governed by fixed processors distributed over several nodes.

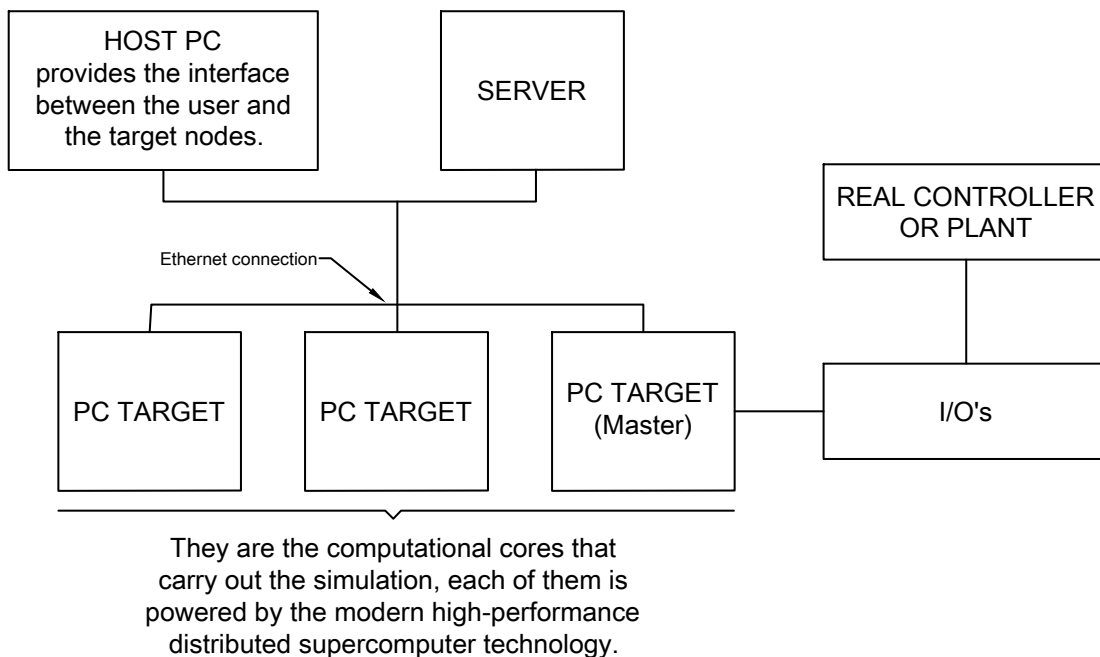


Figure 4.3: RTS hardware setting.

4.3 Solvers

With the continuous evolution of computational techniques and the growing understanding of electrical power systems complexity, solvers continue to be refined and adapted to meet the demands of modern applications. From open-source libraries to commercial software packages, a diverse array of solvers are readily available. It is crucial to emphasise that the accuracy of simulation outcomes reflects an artificial emulation of the physical system. Therefore, understanding the solver is essential for selecting the most suitable one for the application and interpreting the solutions accurately. A summary of the commercially available solvers is presented in Table 4.1.

	RT-Technologies	OPAL -RT	OPAL -RT
Real-Time Simulator	RT simulator	eMEGAsim	HYPERSIM
Real-Time Platform	RSCAD	RT-Lab	HYPERSIM
Environment	RSCAD	MATLAB/Simulink	HYPERSIM
Solver	Dommel algorithm	SS, SSN, ePHASORsim, FPGA	Dommel algorithm

Table 4.1: Solvers characteristics summary.

4.3.1 Dommel’s algorithm: Topological approach

The Dommel’s algorithm[6] is a general solution method for finding time responses of EMT in arbitrary single or multiphase network with lumped and distributed parameters. The modelling of the power system is based on the nodal approach presented in section 3.1.

In the specific case, the trapezoidal rule is chosen for integrating the ordinary differential equations of lumped parameters; it is simple, numerically stable, and accurate enough for practical purposes. For the branches with distributed parameters an exact solution can be obtained with the method of characteristics by neglecting their losses in order to have integrable differential equation form the D’Alembert dissertation. The branch’s losses could be modelled as lumped resistance at both ends of the line. It’s important to note that the trapezoidal integration method is implicit and single-step, whereas Bergeron’s method³ is implicit and multi-step. Consequently, it’s essential to retain more than one step from the previous history of the iterative algorithm. The simplified algorithm flow chart is reported in figure 4.4.

This algorithm is widely utilized for real time simulations. RT-Technologies initially implemented it within its property programming environment **RSCAD**, followed by Opal-RT with its dedicated environment **HYPERSIM**.

4.3.2 State Space (SS)

Besides nodal methods, another very common and widely used family of EMT modeling approaches is the one based on state-space representation.

The commonly used integration methods include the Euler forward, Euler backward and the Trapezoidal rule. It’s important to note that electrical systems often

³The Bergeron method is well-suited for analyzing line reflections in transient phenomena, in contrast to the alternative lattice method for traveling wave phenomena it offers important advantages; for example, no reflection coefficients are necessary when this method is used. It originates from the integration of the D’Alembert dissertation.

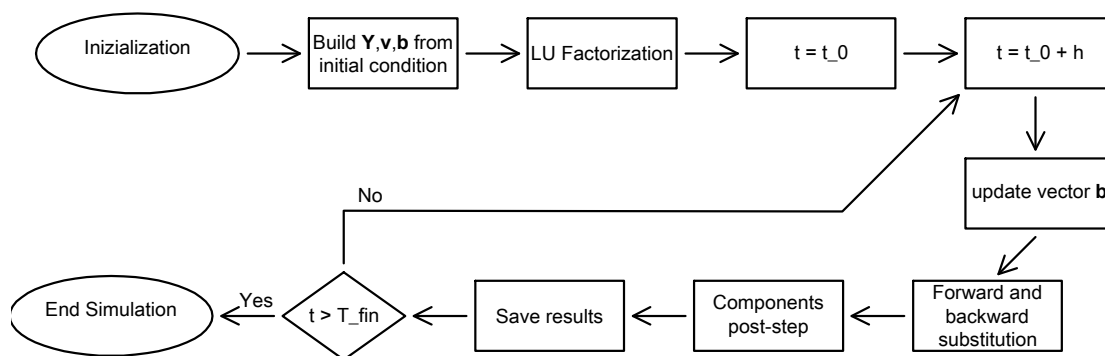


Figure 4.4: Dommel's algorithm flow chart.

necessitate implicit integration (see section 1.3.2 and 2.1.1), making only the last two methods suitable for the task. The system resulting from the discretization is presented in equation 3.6 and equation 3.7. It should be observed that the time instant to which the input vector refers is determined by the specific integration method applied.

Opal-RT has implemented this algorithm within **RT-Lab**, which operates on the MATLAB-Simulink programming environment.

4.3.3 State Space Nodal (SSN) approach

Another approach, for finding time responses of EMT, is presented by the SSN. This simulation method combines state-space analysis (see section 4.3.2) with a nodal method (see section 4.3.1). The advantages observed with this type of algorithm are as follows.

- The nodal admittance matrix can be constrained in size while still permitting the solution of a switched network by nodal admittance matrix on-line triangularisation.
- The state-space formulation enables the use of higher-level discretization methods with L-stability properties (see section 2.1.1).
- The approach enables the coupling of complex nodal-based models like FD-line⁴ into a state-space based solver.

The method work with electrical elements clusters of arbitrary size. The discretization of state equations within the state-space approach typically involves employing

⁴Frequency dependent line.

the trapezoidal rule. The resulting admittance matrix derived from each group of elements, \mathbf{Y}_c , is then mapped through its respective nodes and integrated into the global nodal admittance matrix \mathbf{Y} in order to write the system:

$$\mathbf{Y}\mathbf{v}_{(t+h)} = \mathbf{i}_n(t+h) \quad (4.1)$$

where the vector \mathbf{i}_n contains known nodal current injections, and the vector \mathbf{v} is the vector of all unknown node voltages.

A significant advantage of the method is its ability to efficiently and with low computational and memory costs handle changes in the network's topology. In fact, it's possible to pre-calculate all possible sub-matrices of each group and reconstruct the main matrix \mathbf{Y} at each switch command. In figure 4.5 are reported the solution steps.

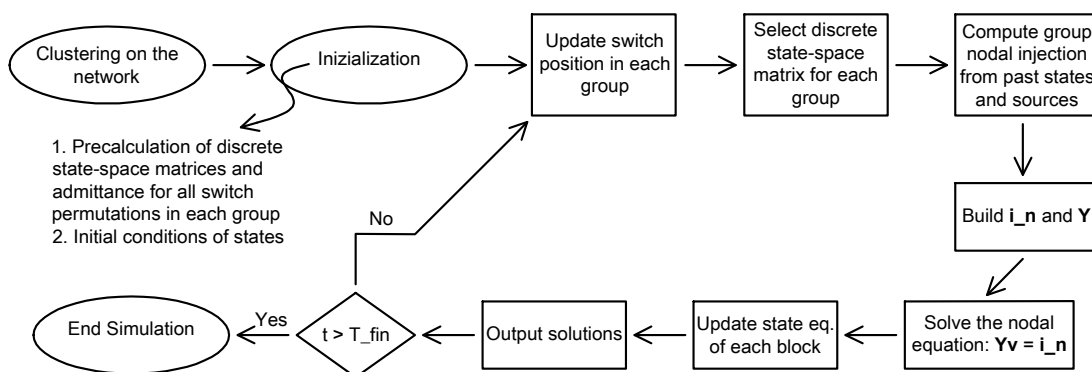


Figure 4.5: SSN flow chart.

The method is implemented in a commercial real-time simulation software tool, the **Advanced Real-Time Electro-Magnetic Simulator (ARTEMIS)** developed by Opal-RT.

4.3.4 Phasor Domain: transient simulation

The massive penetration of small but geographically Distributed Generation (DG) has changed the dynamics of distribution networks. A disturbance in a distribution system within the context of large DG penetration can no longer be considered an insignificant local event. In order to predict the system's response to significant disturbances, potentially leading to substantial fluctuations in rotor speeds, power angles and power transfers, conducting transient stability analysis of the network becomes crucial. Transient stability, being a rapid occurrence governed by electromechanical dynamics, typically manifests within a few seconds. This type

of analysis, due to the time domain involved and the large scale network to be modeled, is not trivial to simulate in real time.

The phasor domain approach is designed for swift and effective transient stability analysis of large-scale systems, specifically tailored for balanced transmission-level networks, where the positive sequence modeling⁵ suffices for analyzing transient stability phenomena. However, since the solver operates in the phasor domain, outputs are provided as RMS value and angle, resulting in a loss of information such as traveling wave effects, transformer saturation, and power electronic device switching. The system is described differential-algebraic equations as follows:

$$\dot{\mathbf{x}}(t) = f(\mathbf{x}, \mathbf{v}) \quad (4.2)$$

$$\mathbf{Y}\mathbf{V} = \mathbf{I}(\mathbf{x}, \mathbf{v}) \quad (4.3)$$

$$\mathbf{x}(t_0) = \mathbf{x}_0 \quad (4.4)$$

where \mathbf{x} is the vector of state variables, \mathbf{V} and \mathbf{I} are the phasorial voltages and currents vectors, \mathbf{Y} is the nodal admittance matrix of the network, and \mathbf{x}_0 is the initial values of state variables. Equation 4.2 describes the dynamic behaviour of the system, while equation 4.3 describes the network constraints on equation 4.2. Each component in the system (except the controllers) is represented in the network's \mathbf{Y} matrix by its primitive admittance matrix (\mathbf{Y}_p). The size of \mathbf{Y}_p depends on type of system modeling and type of the element. For dynamic simulation, the power system is modeled in the main frequency phasor domain, and the dynamics of the system only depend on rotating machines and control devices such as excitation systems, power system stabilizers, turbines and governors. Therefore, a simulation time-step in the order of few milliseconds to half of a cycle is sufficient.

ePHASORsim is a tool offered by Opal-RT and developed in the RT-Lab environment. In the tool the Modified Euler integration method with one iteration of prediction and one of correction at each time-step has been used.

4.3.5 Field Programmable Gate Array (FPGA) based

The real time simulation of fast power electronic systems and controllers is problematic because the ultra rapid dynamic to be reached. It is not uncommon today

⁵The basic idea is that an asymmetrical set of M phasors can be expressed as a linear combination of M symmetrical sets of phasors by means of a complex linear transformation. Fortescue's theorem (symmetrical components) is based on superposition principle, so it is applicable to linear power systems only, or to linear approximations of non-linear power systems. In the most common case of three-phase systems, the resulting "symmetrical" components are referred to as direct (or positive), inverse (or negative) and zero (or homopolar).

to have motor drive controllers with sample times below $25\mu s$ and Pulse Width Modulation (PWM) frequencies well above 20 kHz. The implementation of accurate HIL fully numerical simulators for fast power electronic systems is very challenging. It requires:

- very low-sample time to simulate fast electromagnetic transients caused by power device switching;
- the necessity to sample the IGBT gate signals with high resolution much better than one microsecond;
- to minimize the latency between the firing pulse signals generated by the controller under test and the voltage and current signals send back to the controller.

Consequently several HIL simulator manufacturers and universities are developing fast simulators using FPGA chips or other specialized processor technologies to achieve the required time step values often below 500 ns. Opal-RT **Electric Hardware Solver (eHS) FPGA solver** [7] main objective is to hide the complexity of FPGA programming to control and simulation specialists by providing them an easy-to-use but very powerful and accurate simulation tool. The main solver's characteristics are:

- uses nodal method with fixed admittance matrix to solve switched electric circuits.;
- use the Backward Euler method to provide very good accuracy and stability with time step below 1 microsecond;
- is not limited by the number of switches in the simulated circuit because of the use of constant admittance matrix approach;
- can be interfaced with RT-LAB multi-core power grid simulator with time step below $10\mu s$ to analyze the interaction between the power electronic and grid components.

4.4 Challenges

Despite its advantages, RTS presents several challenges. Ensuring that the simulation remains synchronized with real-world time requires sophisticated hardware and efficient algorithms capable of handling high computational loads. Moreover, achieving low latency and high throughput demands optimized data processing techniques and robust system architecture. Additionally, RTS must often operate

in conjunction with physical systems, requiring seamless integration and communication between virtual models and real-world devices. This can involve complex interfacing and data exchange protocols, adding to the complexity of the simulation setup.

4.4.1 Time step

The real time solvers work always with a fixed time step (figure 4.1) since a change of the time step implicate a recalculation of the LU factorisation of the admittance matrix, so a important increment in the computational burden. Thus is important the selection of the fixed time step to be used for the entire simulation.

The time step is dictate by the frequency of the highest transient to simulate. According to the rule of thumb the simulation step should be smaller than 5% to 10% of the smallest time constant of the system. A smaller time step may be required to maintain numerical stability of stiff systems, unless an A-stable or a L-stable integration method is used (see section 2.1.1). The number of IO channels required to interface the simulator to a real controller for HIL applications is also a critically parameter. Additionally, the system's complexity and the possible change of topology must be taken into account, as a more intricate system imposes a heavier computational burden.

A simulation step that is too large may compromise the accuracy of the solution. This can lead to situations where the method fails to converge. For instance, in simulations of power electronic devices with dynamics exceeding 10 kHz, a time step below $1\mu s$ or the implementation of interpolation algorithms may be necessary. Additionally, compensation measures are required to address jitter resulting from switching between time steps.

At the lower limit of the time step lies the risk of simulation overrun. If the selected time step is too small the computation time may exceed the time step, in this case an overrun error interrupt the simulation.

4.4.2 Stiffness

The theme of stiffness has already been discussed in sections 1.3.2 and 2.1.1. It is important to note that in the context of RTS solvers, explicit methods such as the forward Euler method can never achieve A-stability, whereas implicit methods are better suited for handling stiff problems. For instance, the trapezoidal rule is A-stable, and the backward Euler method is L-stable. To note that employing more power integration methods, which can make the integration of an unstable system (by nature stable), may lead to serious simulation artifacts.

Newer discretization methods as emerged like the order-5 L-stable discretization rules of ARTEMIS-SSN (see section 4.3.3). Because of its higher order, ARTEMIS order-5 can be more accurate than order-2 solver (only A-stable) for the same time step value. Such features enable the use of larger time step values, which facilitate real-time simulation of difficult cases.

4.4.3 Jitters

In real-time simulation systems, the occurrence of jitters is unavoidable. These delays can significantly impair control performance, introduce simulation artifacts, and in some cases, lead to instability. Managing these jitters poses considerable challenges when incorporating a Hardware in the Loop routine. It's crucial to note that despite this issue, the entire routine must adhere to the fixed time step selected for the simulation to prevent overrun.

Overall, we have three different cases to consider (see figure 4.6).

1. **Sampling jitter**, with negligible controller execution time: time intervals between consecutive sampling points (h_m) are not constant.
2. **Sampling-actuation delays** with strictly periodic sampling, with negligible controller execution time: samples are taken at periodic times (via interrupts, for example). Control computations suffer from start time jitters. As a consequence, actuation instants are not strictly periodic, and this results in varying sampling-actuation delays (Δt).
3. **Sampling jitter** with significant controller execution times: time intervals between consecutive sampling points (h_m) are not constant, which results in sampling jitter. In addition, control computations suffer from start time jitters and may have varying execution times. As a consequence, actuation instants are not strictly periodic, which results in varying sampling-actuation delays (Δt).

In these three cases the delays determine a violation of the constant sampling or equidistant actuation assumptions. In case 1 sampling jitter is present, violating the constant sampling assumption. In case 2, sampling-actuation delays occur, violating the equidistant actuation assumption. Finally, in case 4, both sampling jitter and sampling-actuation delays occur (and made worse due to varying execution times), which is a combination of the previous two problems.

It's crucial to consider these latencies when modeling systems to mitigate their effects on simulation outcomes (for example using FPGA chips), particularly when dealing with high-frequency systems ($>10\text{kHz}$), such as those in power electronic applications. Solvers, in turn, can deploy compensation techniques such as those

outlined in [8].

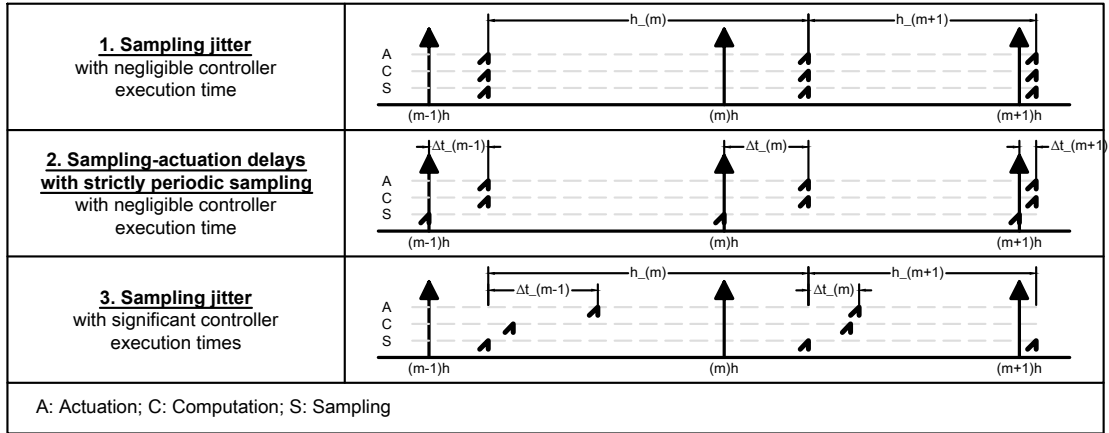


Figure 4.6: Jitters summary.

4.4.4 Non linearities

In presence of non linear components the possible approach are two.

1. Linearizing the nonlinear component around the system's operating point, accepting the resulting decrease in accuracy.
2. Adding an internal loop to the procedure complements the external loop governed by the specified timeline (iterative procedure). This internal loop is essential for updating all nonlinear component contributions at each iteration, along with the nodal solution being repeated until a predefined tolerance is achieved.

While the second method yields a more precise solution, its applicability to real-time simulations is severely constrained. Primarily, the internal loop necessitates the recalculation of the admittance matrix \mathbf{Y} multiple times within each time step, preventing the offline factorization of the matrix. Additionally, while the number of iterations in the external loop can be accurately predicted based on the final simulation time and step size, the number of iterations in the second loop varies depending on the desired accuracy and specific operating conditions, making it impossible to define beforehand.

In Figure 4.7 is reported the non linear resistive companion flow chart from [3] to aid the comprehension.

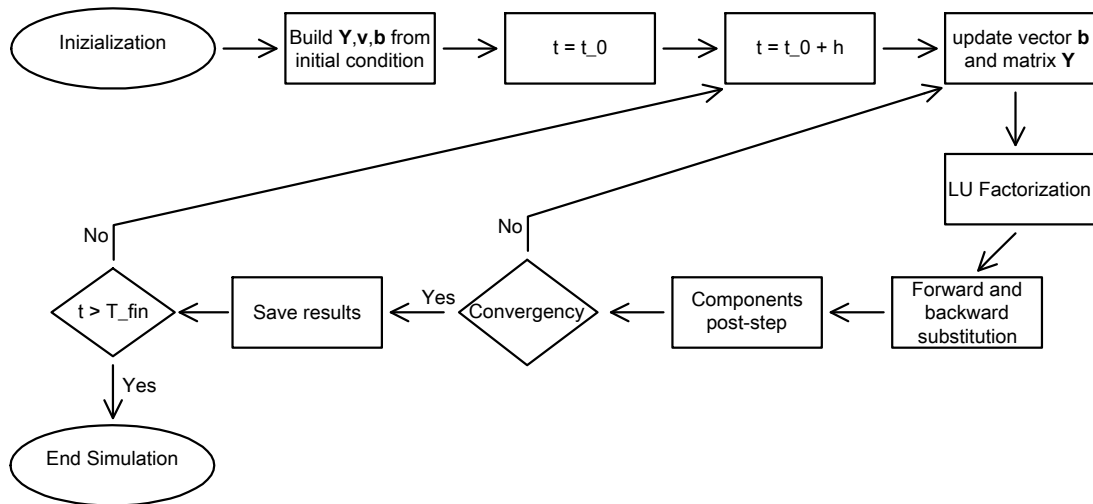


Figure 4.7: Non linear resistive companion flow chart.

4.5 Performances

In this section is reported in Figure 4.8 a summary highlighting the key performance aspects of the depicted solvers. It's worth noting that to enhance their simulation capabilities, one can consider implementing the following technological measures:

- Parallel processing operation on different CPU to split the calculation burden;
- Multi-rate simulation to take full advantage of modern processor technologies, and therefore offer maximum accuracy over a very wide frequency spectrum;
- Multi-domain capability enables the simulation of each class of component with an optimal solver for each specific class;
- Co-simulation to process the system on different simulators.

SOLVER	MODELLING	INTEGRATION
Dommel	Nodal	Trapezoidal + Bergeron
SS	State Space	Euler Backward, Trapezoidal
SSN	State Space / Nodal	Trapezoidal
ePHASORSim	Nodal	Phasor domain
FPGA	Nodal	Euler Backward

Table 4.2: Solvers modeling summary.

ePHASORsim (Opal-RT)	Phasor domain simulation (transient stability simulation)	seconds	Large 10000 plus nodes	- Distribution systems - PMUs, SCADA and cyber security development - large distribution system simulation
HYPERSIM (Opal-RT)	Large scale EMT simulation (Dommel's solver)	Mili seconds	Small less than 100 nodes	- Transmission and distribution simulation - Fast transient simulation, controller testing and protection studies
EMEGAsim (Opal-RT)	Modelling based on Matlab/Simulink (State space solver)	Micro seconds	Small less than 100 nodes	- Possibility to hybrid simulation (SSN solver) - Power system and power electronics simulation - Micro grid applications and control algorithms development
eFPGAsim (Opal-RT)	Adapted nodal method	Nano seconds	Small less than 100 nodes	- Fast power electronics simulation on FPGA - Drivers controller development - Modulat multilevel converters controller development
RSCAD (RTDS - Technologies)	Large scale EMT simulation (Dommel's solver)	Micro seconds	Small less than 100 nodes	- Transmission and distribution simulation - Fast transient simulation, controller testing and protection studies

Figure 4.8: Solvers performance.

Chapter 5

Model presentation

The growth of the RES quote on the distribution grid, alongside or in substitution of the traditional power plants (based on a turbine-generator coupling), introduced the new conception of Low-inertia Power System. A Low-inertia Power System (figure 5.1) is an electrical system of interconnected power generators in which the global inertia, inherently provided to the system via the rotating parts of synchronous generators, is reduced consistently introducing "static" RES generation [9]: generation connected to the grid by means of power converter in order to adapt the frequencies of the produced energy to the reference value of the power system (theoretically known as Center Of Inertia). Inertia is a useful mechanism to front supply/demand imbalances or contingency events, making available a reserve of kinetic energy that can be instantaneously converted into electrical power. It guarantees to grid operators a time window to respond with an adequate action (with power/frequency controls) to maintain the system stability and align the mechanical power production of plants to the electrical power requested. A reduction of the global power system's inertia results in an increase in the Rate Of Change Of Frequency (ROCOF) of the system while facing load unbalances. A greater deviation of the frequency in a short period of time is a threat to the frequency stability of the power system, as ROCOF protection relays might trip, isolating some generators and increasing the difference between supply and demand [10].

The arise of aforesaid problems requires new solutions to properly control the frequency stability of low-inertia power systems. The necessity of new ways to create additional inertia in the system is also important to make possible the global energy transformation that will lead grids all over the world to an even greater penetration of RES. The integration of virtual inertia into the power system is currently the solution that inspires the most confidence and attracts the

greatest investment. It is implemented by increasing the number of Energy Storage System (ESS) installation on the grid: energy storage interfaced with converters controlled to behave in an equivalent way to normal rotating generators, providing an inertial response to frequency variations. There are many different technologies for ESS:

- pumped storage power plants;
- supercapacitors;
- electromechanic energy storage;
- Superconducting Magnetic Energy Storage (SMES);
- battery energy storage.

Currently, the most actively developing ESS are BESS: they are not limited to the installation site, ensure quick response (at the rate of transients in power systems) and have acceptable technical and economic characteristics.

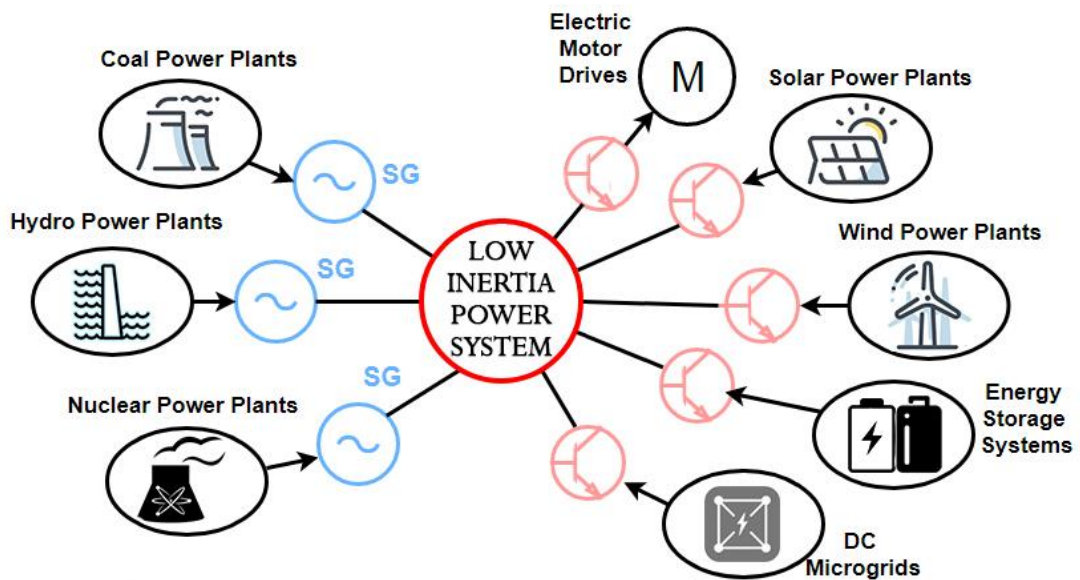


Figure 5.1: Low-inertia Power System [10].

The model presented here will serve as the foundation for the RTS of scenarios aimed at gaining a deeper understanding of the dynamic responses in low-inertia power systems and to assess the efficiency and impact of virtual inertia systems,

such as BESS, on the overall power grid. Here lie the foundations for the creation of a digital twin of the electrical grid.

5.1 Topology: Rural Net

The reference topology is derived from the Archivio TeLemAtico per il riferimento Nazionale di reTI di Distribuzione Elettrica (ATLANTIDE) which stands for “Digital Archive for the National Electrical Distribution Reference Networks”[11] and contains reference models of both passive and active distribution networks. The model used is "ATL-WP2-LA2-ANX-R01" in its "clustered" version, designed to reduce the network size by merging the nodes of the original network and considering only the Medium Voltage (MV) nodes. The model is based on an Italian rural network as the reference.

The swing node, "node 0," is a High Voltage (HV) node operating at 150 kV. It represents the behavior of the Italian electrical system as viewed from the modeled portion of the distribution network. All nodes within the distribution network are at MV level, specifically 20 kV, with no Low Voltage (LV) nodes present. A three-phase transformer rated at 150/20 kV and 25 MVA, "node 1," connects the swing node to the distribution network composed by 7 feeders.

The resultant network, schematically represented in Figure 5.2, has the following characteristics:

- the total number of MV nodes is 103;
- the nodes are supplied by 7 feeders;
- the total line length is 157456km;
- the power absorbed by the network’s loads is 18.14MVA.

5.2 Dynamic generation

The zero node serves as the model’s swing node and is the only HV node. It represents the behavior of the Italian electrical system from the perspective of the modeled section of the MV distribution network. This node must supply power to all distribution nodes, except for the portion provided by distributed generation sources, such as photovoltaic systems.

The node is modeled as a dynamic generation source, specifically as a synchronous machine. This allows it to simulate the dynamic response during transients and generate the necessary power to supply the connected loads. Although the network’s

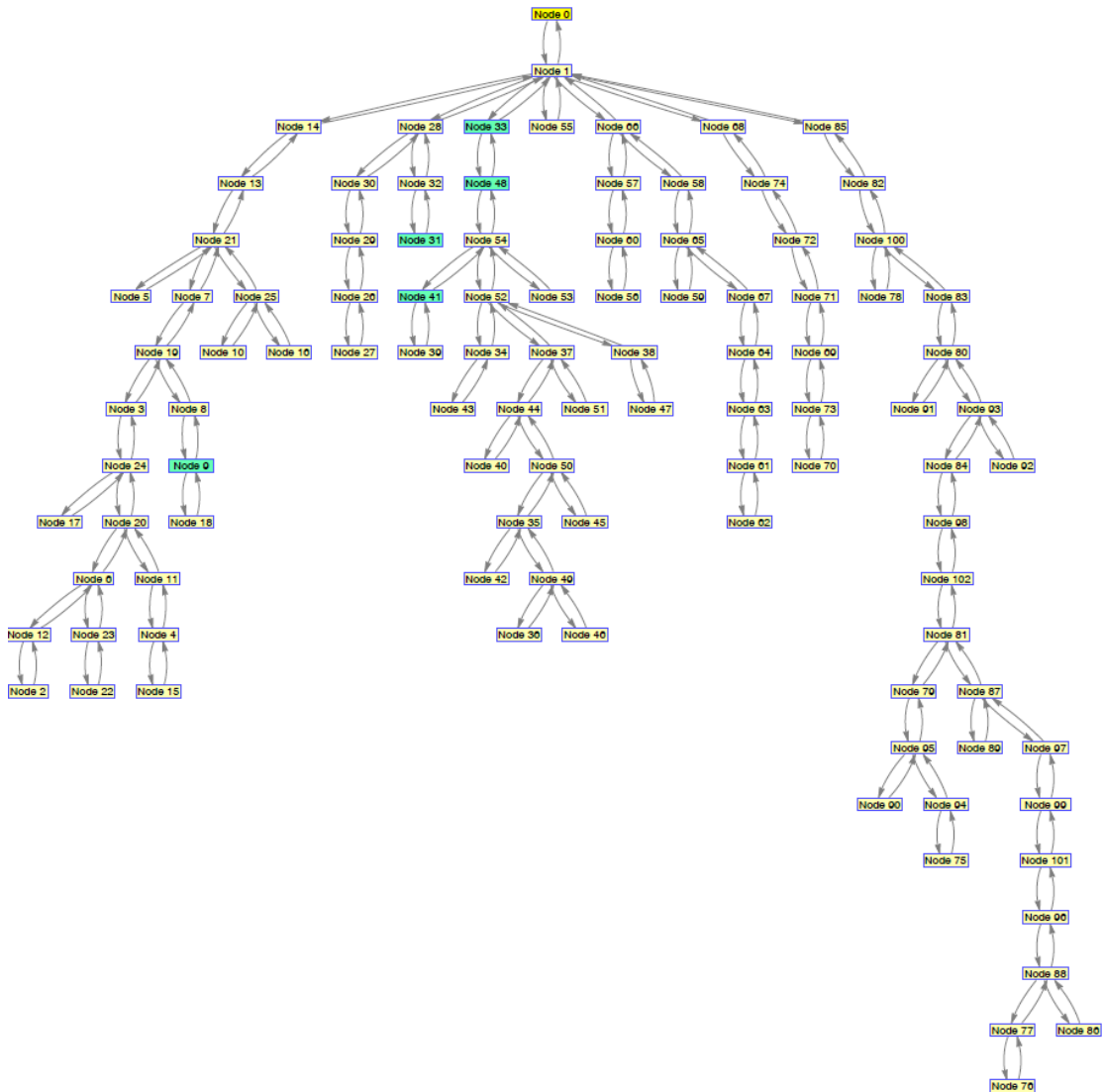


Figure 5.2: Model’s topology: Rural net.

total load is approximately 20 MVA, the generation has been intentionally oversized (hundred of MVA) to accurately represent the entire Italian system and its inertia within a single node.

5.2.1 Simulink model

The Simulink model of the swing node is shown in Figure 5.3. The power components are as follows:

- the synchronous machine;
- the excitation system;
- the steam turbine and governor.

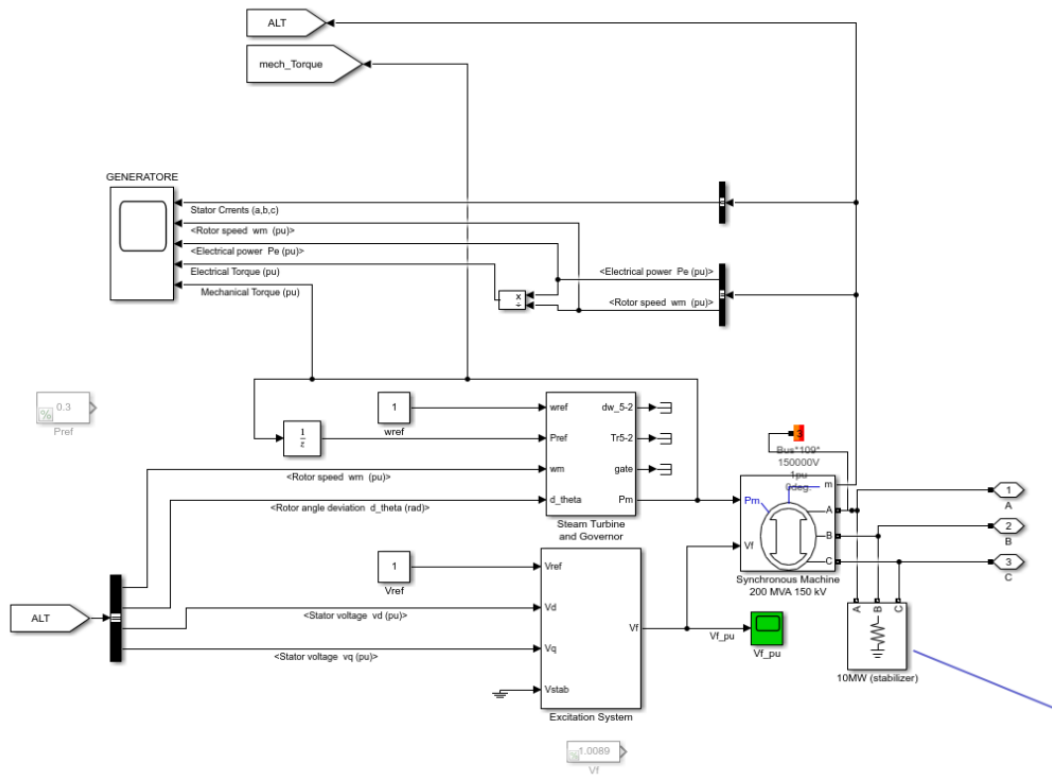


Figure 5.3: Dynamic generation Simulink model.

The synchronous machine block is a Simulink component that implements "a 3-phase synchronous machine modeled in the dq rotor reference frame. The stator windings are wye-connected to an internal neutral point". The rotor type is a salient pole, with a rated voltage of 150 kV and a rated power of 200 MVA. The excitation system block implements an IEEE Type 1 synchronous machine voltage regulator combined with an exciter, it supplies the field voltage to the synchronous machine. Lastly, the steam turbine and governor block represent a complete tandem-compound steam prime mover system, including a speed regulator, steam turbine, and a shaft with up to four masses. The return of output "Pm" to the input "Pref", with the inclusion of a "unit delay block" to prevent a simulation loop and introduce the initial power supply from the load flow analysis of the entire model, is crucial for achieving a null speed deviation when the system returns to

steady state at the end of the dynamic simulation.

It is essential to adjust the parameters of the turbine and governor block to achieve an optimal transient response for the simulation's objectives. Since the generator is intended to model the entire HV Italian transmission network, its parametrization must be customized rather than using a standard synchronous generator. This process was carried out manually through iterative adjustments, fine-tuning the parameter set until the desired transient response to a load step was achieved.

The 10 MW parasitic resistive load, connected at the machine terminal, is required to prevent numerical oscillations. With a sample time of $50\mu s$, the Simulink manual recommends using approximately 5% of resistive load.

5.3 Connection elements

Connection elements of the network are: power lines and transformers. The distribution connections are MV overhead lines, operating at $20kV$, commonly used for distribution in rural areas. An overhead power line is a structure used in electric power transmission and distribution to carry electrical energy over long distances. It typically consists of multiple conductors (often in sets of three) suspended by towers or poles. Overhead power lines are favored because the surrounding air provides effective cooling and insulation over long distances, and allows for visual inspections. They are generally the most cost-effective method for transmitting large quantities of electric energy. Support towers for these lines are typically made from materials such as wood (natural or laminated), steel, aluminum, and occasionally reinforced plastics. The conductors on these lines are typically made from aluminum (plain or reinforced with steel), or composite materials like carbon or glass fiber. Copper wires are used less frequently due to their higher cost. Power grid transformers are a crucial component in electrical power systems, used primarily for stepping up or stepping down voltage levels to facilitate efficient transmission and distribution of electrical energy. They are fundamental to interconnect power grids operating at different voltage level. Step-up transformers increase voltage from a lower level to a higher level, typically for long-distance transmission to reduce energy losses. Step-down transformers decrease voltage for distribution and end-user consumption. Transformers are designed to operate efficiently with minimal losses. They are critical components of the grid infrastructure, requiring regular maintenance and monitoring to ensure reliable operation. Large transformers often must incorporate cooling systems, such as oil or air cooling, to dissipate heat generated during operation. This ensures they operate within safe temperature limits and maintain their efficiency. In the model, there is a single machine used to connect the HV swing node to the rest of

the distribution network at MV. This machine has a Dyn winding connection and a 11 vector group configuration. Its rated power is 25 MVA.

5.3.1 Simulink model

The connection lines are modeled using the "Three-Phase PI Section Line" block in Simulink. This block simulates a three-phase transmission line with a single PI section. The model consists of one set of RL series elements between the input and output terminals, along with two sets of shunt capacitances lumped at both ends of the line. The transformer is modeled using the "Three-Phase Transformer (Two Windings)" Simulink block. This block implements a three-phase transformer by using three single-phase transformers. The used blocks are shown in Figure 5.4.

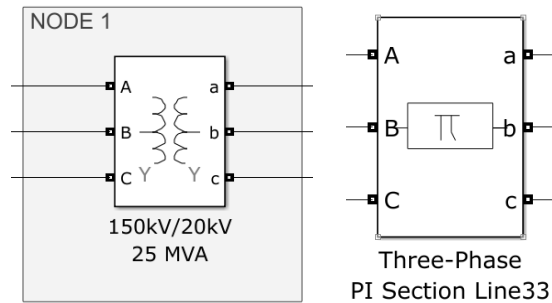


Figure 5.4: Simulink model of the connection elements.

5.4 Loads and distributed generation

At every node in the network, a load block aggregates all the energy absorption and generation activities for that specific section of the network. This modeling approach simplifies the simulation by summarizing all activities related to LV distribution and MV utilisation, which are not explicitly detailed. In the simulation, the standard load absorbs 18.14MVA. In the different scenarios, which will be implemented, this value will vary by the addition of distributed generation and the application of load steps to observe the system's dynamic response.

5.4.1 Simulink model

The load block is implemented using three "Three-Phase Dynamic Load" Simulink blocks connected in parallel to create a ZIP load model. Each of these blocks represents the "Z", "I", and "P" components of the ZIP model:

- Z component represents the impedance-related characteristics of the load;

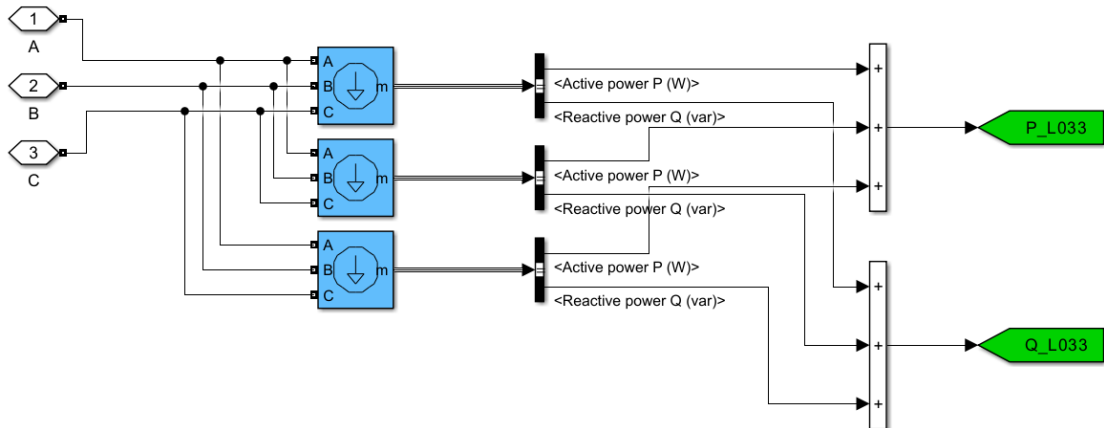


Figure 5.5: Dynamic ZIP load Simulink model.

- I component represents the current-related characteristics of the load;
- P component represents the active power-related characteristics of the load.

By combining these three blocks in parallel, the ZIP load model can simulate the complex behavior of real-world loads, taking into account their impedance, current, and power characteristics simultaneously. This approach provides a more realistic representation of how loads interact with the electrical network under varying conditions and helps in studying the system's response to different scenarios in the simulation. In this case, only the "P" component is activated to simplify the simulation, indicating that the load behaves like a constant power load. The "Z" and "I" components are deactivated by setting their values to zero in their respective blocks. This simplification assumes that the load's impedance and current characteristics do not vary significantly, focusing primarily on its active power consumption.

To simulate a generation quota in the network using the load block, you can achieve this by adding a negative power quota to the respective load block. This approach effectively represents the injection of power into the network, simulating the behavior of a generating source rather than a consuming load.

5.5 Battery Energy Storage System

A Battery Energy Storage System or battery storage power station is a type of ESS that uses a group of batteries to store electrical energy. Battery storage is the fastest responding available source of power on electric grids and it is used to stabilize those grids, as battery storage can transition from standby to full

power in under a second to deal with grid contingencies. They can be used for short-term peak power and ancillary services, such as providing operating reserve and frequency control to minimize the chance of power outages. They are often installed at, or close to, other active or disused power stations and may share the same grid connection to reduce costs. Since battery storage plants require no deliveries of fuel, are compact compared to generating stations and have no chimneys or large cooling systems, they can be rapidly installed and placed if necessary within urban areas, close to customer load.

In table 5.1 are reported the five largest battery storage power plants by storage capacity in the world. The use of this type of system is becoming increasingly widespread, and in the future, larger installations will likely be implemented. In figure 5.6 it is presented the general scheme of a BESS connected to grid. The battery storage is interfaced via a bidirectional buck-boost converter which controls the charge discharge processes during severe operating condition such as fault occurrences. From the G-VSC¹ AC output terminals, the hybrid subsystem is connected to the utility grid at the Point of Common Coupling (PCC) through a low-pass filter and an interconnection transformer that are represented by an inductor. These components are responsible for filtering harmonics and isolating the entire system from the utility grid.

Name	Energy [Mwh]	Duration [h]	Type	Location
Edwards Sanborn	3284	N/A	Li-ion	California
Vistra Moss	3000	4	Li-ion	California
Gemini	1416	4	Li-ion	Nevada
Crimson	1400	4	Li-ion	California
Desert Peak	1300	4	Li-ion	California

Table 5.1: Five largest battery storage power plants by storage capacity.

5.5.1 Simulink model

The BESS's model is divided in three main subsystem:

- the power subsystem (in orange);
- the control subsystem (the first in blue);

¹Grid-side Voltage Source Converter. To inject electrical power efficiently and safely into the grid, grid-side inverters must accurately match the voltage, frequency and phase of the grid sine wave AC waveform.

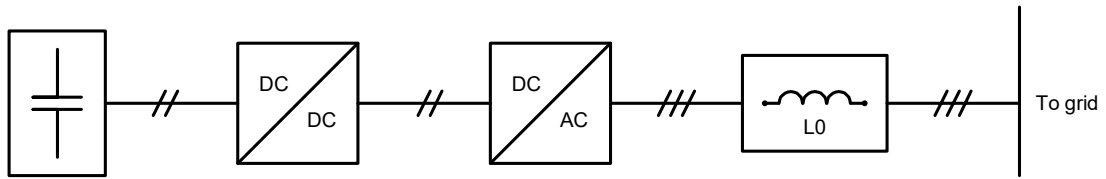


Figure 5.6: BESS general scheme.

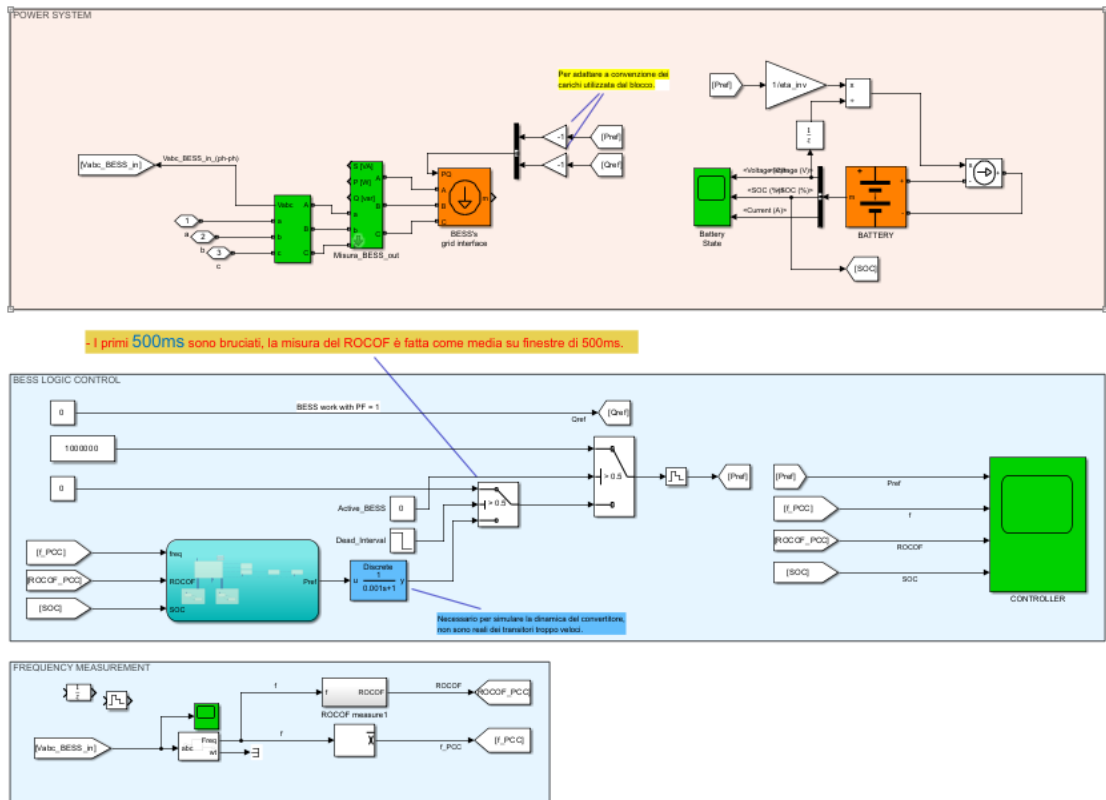


Figure 5.7: BESS Simulink model.

- the measurement subsystem (the second in blue).

To minimize computation time when studying long electromechanical transients, the power subsystem is developed without detailed transistor converter models. Instead, the output terminals are modeled using a three-phase controlled power source: the Simulink block generates the active and reactive power at the output terminals, as requested by the control subsystem. The Lithium-Ion battery model is implemented using the dedicated Simulink block. To simulate the energy absorption

or supply in the battery model and update both the SOC and battery voltage, the terminals are connected to a controlled current source. This source adjusts the current to reflect the power flow into or out of the battery. The current is determined by dividing the power requested (with its corresponding sign) by the voltage at the battery terminals, considering a conversion efficiency of 95%.

The outputs of the control subsystem are the active and reactive power that the BESS must supply to or absorb from the grid. In the model, these are referred to as "Pref" and "Qref" because, in a real system, they represent the reference power values provided to the power converter that interfaces the batteries with the grid. The implemented control strategy aims to provide a fast frequency response, considering a MW-scale BESS installation. The power factor is kept at unity by maintaining the exchanged reactive power at zero, while the active power is regulated by the control. In the proposed strategy, the SOC is maintained in the specific range in which the life cycle is maximized, the interference of SOC recovery by frequency control is minimized, the responding capacity for providing the virtual inertia response is maximized during the transient period, and the performance requirements for frequency response are satisfied. The control strategy implemented to manage the active power output is illustrated in Figure 5.8, while the recovery control of the BESS based on SOC ranges is shown in Figure 5.9. For more detailed information, please refer to [12].

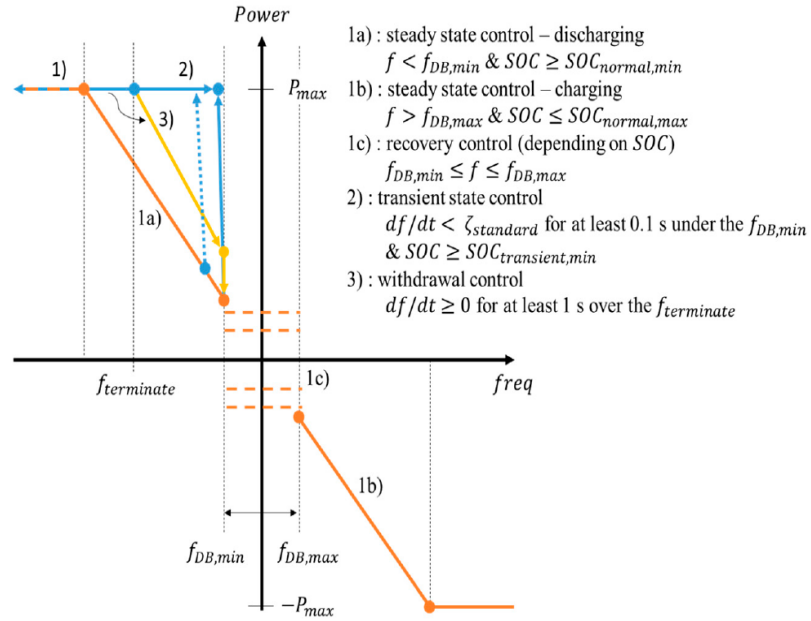


Figure 5.8: Control strategy of the BESS for providing virtual inertia and primary frequency response.

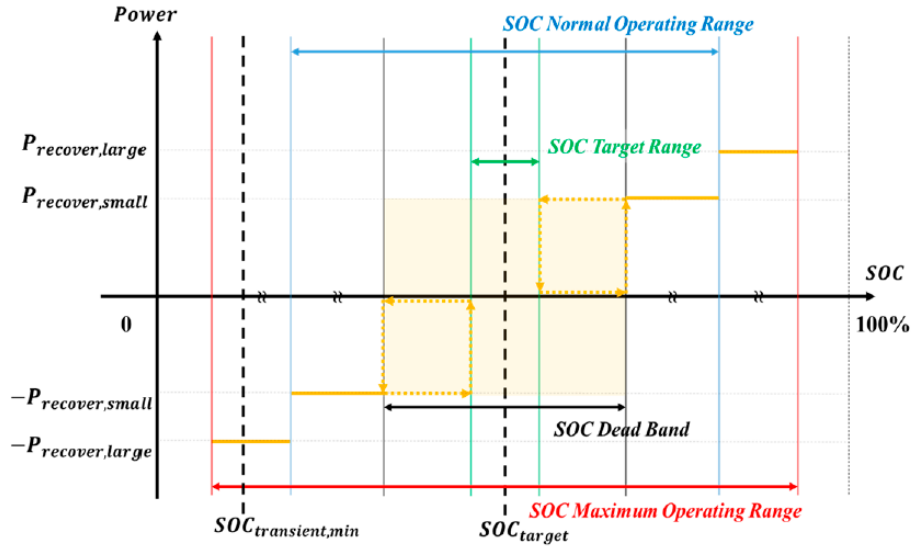


Figure 5.9: Reconvry control of BESS on SOC ranges.

To implement the simulation the speed droop² is set to 4% during steady-state operation and 2% during withdrawal operation. The other control parameters, based on SOC and frequency, are summarized in Table 5.2.

The measurement subsystem is essential for detecting the frequency and ROCOF at the PCC, which are then provided as inputs to the control subsystem. The PLL Simulink block models a Phase-Locked Loop (PLL) closed-loop control system that tracks the frequency and phase of the input normalized sinusoidal signal using an internal frequency oscillator. The control system adjusts the internal oscillator frequency to maintain a phase difference of zero. The ROCOF is essentially the derivative of the frequency. Both the frequency and the ROCOF measurements are filtered to reduce noise. They are averaged over a running window of 40ms and 300ms, respectively.

²Droop speed control is a control mode used for AC electrical power generators, whereby the power output of a generator reduces as the line frequency increases. It is commonly used as the speed control mode of the governor of a prime mover driving a synchronous generator connected to an electrical grid. It works by controlling the rate of power produced by the prime mover according to the grid frequency. With droop speed control, when the grid is operating at maximum operating frequency, the prime mover's power is reduced to zero, and when the grid is at minimum operating frequency, the power is set to 100%, and intermediate values at other operating frequencies. $Droop\% = (NoLoadSpeed - FullLoadSpeed)/NoLoadSpeed$.

Parameter	Value
Frequency dead band	50 ±0.005 Hz
$\zeta_{standard}$	-0.1 Hz/s
$f_{terminate}$	49.9 Hz
SOC maximum operating range	10 - 90 %
SOC normal operating range	50 - 80 %
SOC target range	65±0.5 %
SOC dead band	65±2 %
SOC _{TransientMin}	15 %
Ratio for recovery control	10 - 20 %

Table 5.2: Specifications for operating BESS.

5.6 Emergency Automatic Control relay

The EAC system is typically installed at electrical stations to implement a load-shedding strategy during under-frequency transients. When the frequency at the installation node drops below the threshold value, the system commands the breaker to open, disconnecting the load from the network. This strategy helps to mitigate the severity of the transient, preventing potential blackouts and facilitating frequency restoration.

5.6.1 Simulink model

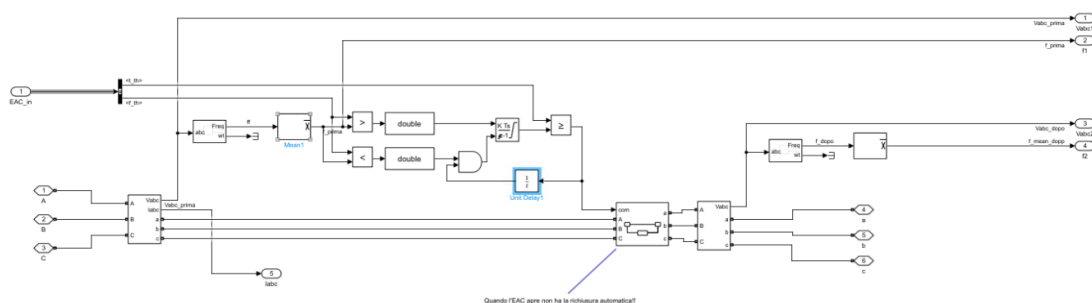


Figure 5.10: EAC simulink model.

The model continuously monitors the network frequency and compares it to the threshold frequency ($f.th$). If the frequency remains below this threshold for at least the specified duration ($t.th$), the breaker is activated, disconnecting the section of

the grid it controls. A resettable integrator in the model ensures that the condition remains true for a specified duration before commanding the breaker. Each time the condition becomes false, the integrator is reset until the breaker is activated. Once the network is opened, the breaker remains in the open position and does not close again for the duration of the simulation.

5.7 Implementation of the simulation in real time

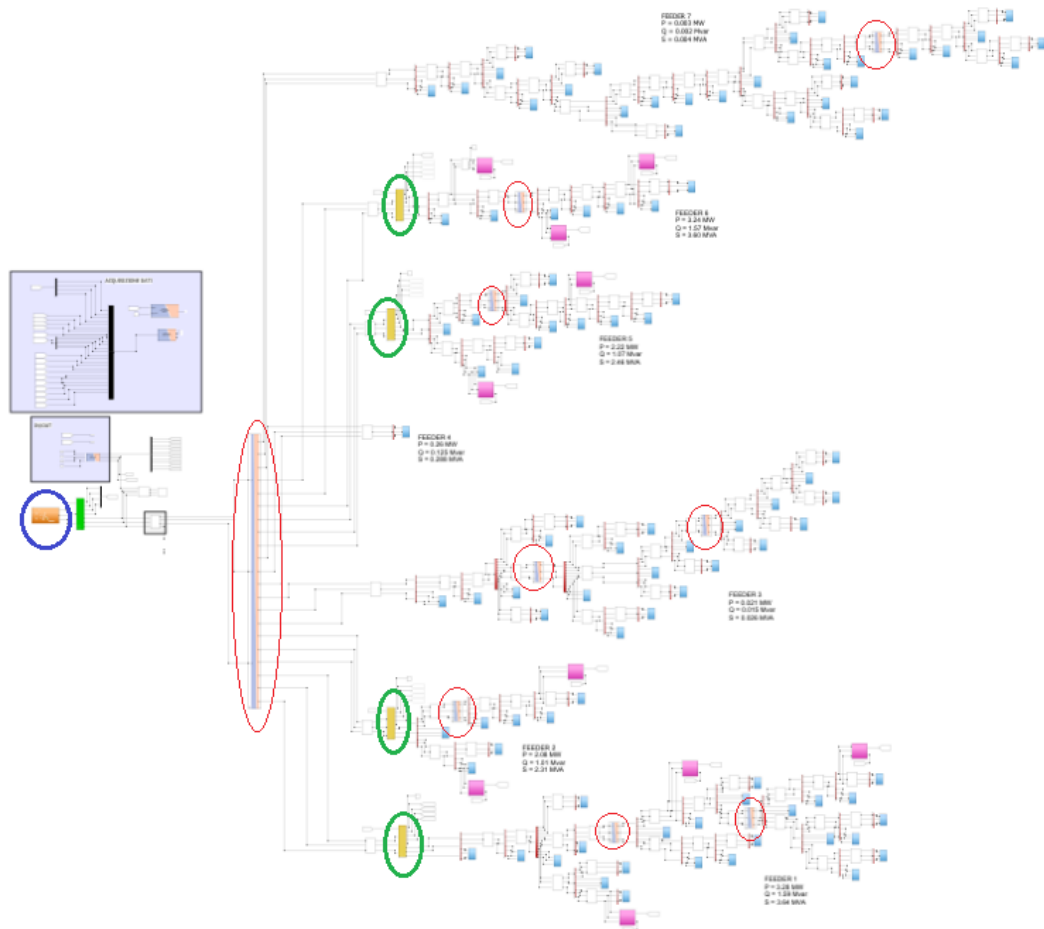


Figure 5.11: Network model in Simulink.

The network topology outlined in section 5.1 is represented in the Simulink model shown in figure 5.11. Within the blue circle is the generation node, which connects to the rest of the network through the high voltage/medium voltage transformer. The seven feeders, numbered from bottom to top, are easily distinguishable as they

disconnect from the main bus. Within the green circle are the EAC relays installed at the beginning of feeders 1, 2, 5, and 6. The same feeders are connected to the BESS, which are highlighted in pink in the model.

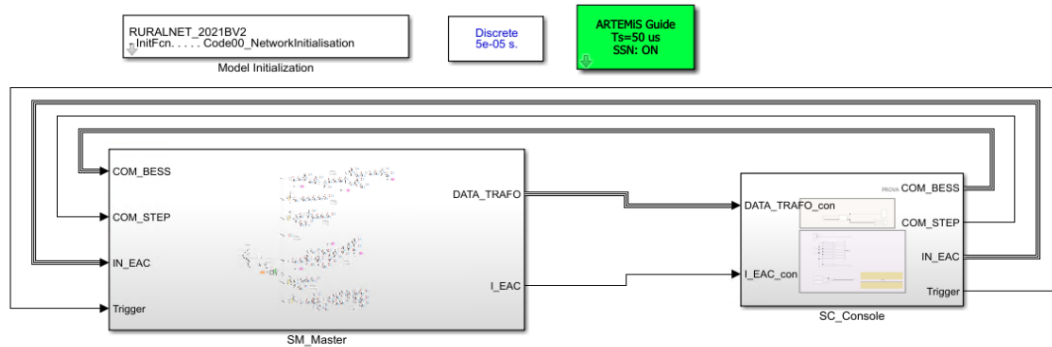


Figure 5.12: Organization of the RTS model in Simulink.

To enable the RTS, the model is structured as shown in figure 5.12. The "SM_Master" block, located on the left, contains the previously described network model, which will be executed in real time by the OPAL-RT simulator. The "SC_Console" block, on the right, will operate from the Windows terminal, allowing for interaction with the simulation, although the execution time will differ from real time.

5.7.1 Decoupling the distribution network for multi processor Real Time Simulation: SSN solver

As modern distribution systems increasingly depend on complex power electronics and the integration of numerous active distributed generation systems, the complexity of the active grid grows. This poses two major challenges for real-time simulation of these systems that any real-time simulator must address:

- the accuracy in simulating switching power converters especially with the tendency of using an increasing switching frequency;
- the ability of the Simulator to simulate large power distributed systems with a large number of components, modules and buses.

The first challenge has already been addressed, as the converters are represented by their mean-value model, as outlined in Section 5.6.1. This section will tackle the second issue: the simulation of large distribution power systems.

The size of distribution networks is one of the major obstructions to perform an accurate and stable Electromagnetic Transient real time simulation. The only way for real-time simulators to be able to simulate them in real-time (to solve all the

grid equations/matrices within the finite simulation cycle) is to split the grid model and distribute it on several processors included in the simulator. However, dividing a power grid model across multiple processors presents a significant challenge due to the additional delays introduced by communication and send/receive overheads. For this reason, in real-time simulator, it is essential to partition the grid model at network elements that naturally exhibit delays, such as inductors, capacitors, and transmission lines. The problem with distribution grids, though, is that they are inherently lumped systems with only short transmission lines (typically 2–5 km).

In this context, it becomes essential to implement the model using the State Space Nodal method [13], described in Section 4.3.3. In SSN, the user partitions the network by introducing "SSN nodes". These partitions are solved using a state-space approach, while the interfaces between groups are handled via a nodal method [14]. When multiple cores are allocated for the system, SSN groups are automatically distributed across the available cores, allowing the partitions to be solved in parallel without introducing algorithmic delays, thus minimizing overall computation time. Additionally, the algorithm automatically computes the network's branch equations and reduces the number of nodes. This node reduction is critical because the time required for LU factorization (see Section 2.2) of the \mathbf{G} matrix increases proportionally to the cube of the matrix size. Thus, the number of groups and their relative size will have a direct impact on the possible performance improvements for the parallel mode.

Figure 5.11 presents the network model implemented in Simulink, with the "SSN nodes" highlighted by red circles. The network has been divided into nine groups: one for each feeder, one for the generation node with the interface transformer, and one for the BESS. These groups will be automatically distributed across the three available cores and simulated in parallel.

Chapter 6

Model simulation

This section presents the implementation of a RTS scenario based on the model introduced in Chapter 5. At the end of the chapter, the simulation results are presented and discussed.

6.1 Hardware description

OP5700 is a real time simulator built by Opal-RT Technologies which simulation software is the RT-LAB. RT-LAB enables rapid prototype since it is an integrated real time software where control system test and HIL simulation can be performed. Opal-RT uses MATLAB (specifically Simulink) as a model editing tool, working as user designing front-end application [15]. The OP5700 architecture is divided in two main sections. In the first section the analogue and digital *I/O* modules are assembled, and the second section is composed by a multi-core FPGA able to run the models of the real time simulation software. The OP5700 can be connected through *TCP/IP* Ethernet to a Windows hosting computer to edit and monitor the simulations [16]. Figure 6.1 illustrates the simulator architecture. OP5700 has 8 slots of *I/O* boards per system. Each analog board has 16 channels and supports up to 128 in the system. Each digital board has 32 channels per slot and support up to 256 per system. Regarding the connectivity, supports Ethernet and RS232. The supported communication protocols for Energy systems are S7, Profibus, Modbus, S7, Aurora, IEC 60870104, DNP3 outstation (slave) and master, ABB PS935 [20]. In this particular case, the simulator's *I/O* interface will not be utilized.

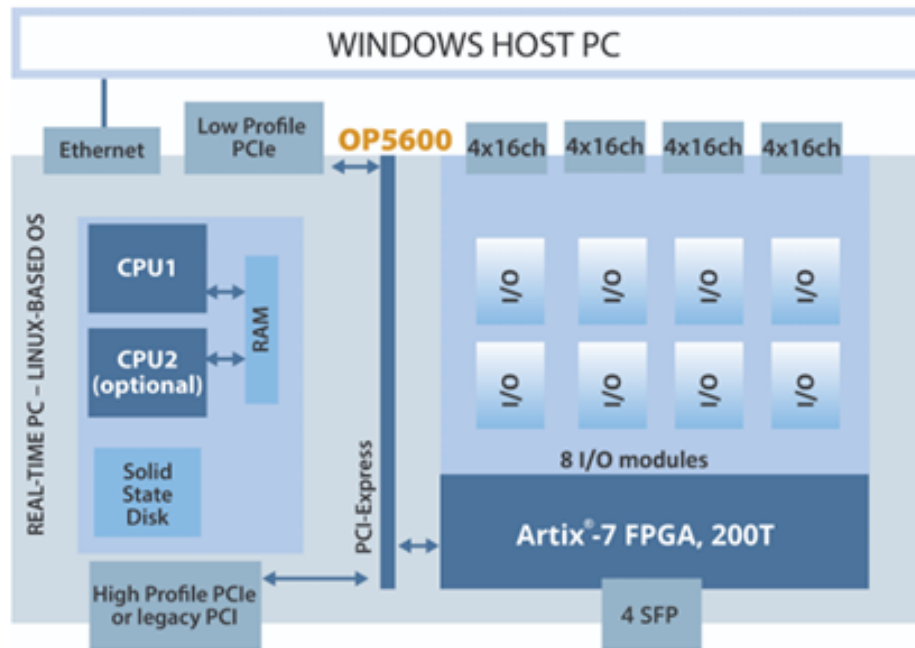


Figure 6.1: Opal-RT simulator architecture [16].

6.2 Scenario description

To ensure a well-structured and comprehensive scenario description, the use case is presented in accordance with the IEC 62559-2 edition 1 standard. For ease of reading, the description is provided in a less tabular format. Follow the implementation of the scenario on the model presented in chapter 5.

6.2.1 Use case

The interest area is the *transmission/distribution* network interaction, in particular the analysis through Digital Twin (DT) of the behaviour of aggregated distributed resources during a grid event in the TSO system. This use case focuses on developing a DT of selected portions of the medium distribution grids, with a particular focus on integrating Distributed Energy Resources (DER), such as photovoltaic systems and electric vehicle charging stations. The objective is to evaluate operational challenges related to load and generation variability, ensuring secure grid operations, especially in high-density urban areas and rural zones. Simulations will be carried out using real time techniques, focusing on the MV network and aggregating data at the MV substation level. The model will run on a real time simulator. The primary goal is to gather data on voltage, frequency, and load profiles, validating

Scope	Analysis of the impact of aggregated distributed resources on the distribution network with the participation of relevant shares of inverter-based resources.
Objective	Studying the impact of inverter-based resource operation on the distribution network after a transmission system grid events.
Related business case	System secure operation.

Table 6.1: Scope and objective of use case.

the simulations based on real data obtained from selected primary substations, the selection will depend on the size of the substation. Afterwards, the study will analyze the behavior of the distribution network when working in (virtual) islanding mode, to understand the impact on the distribution system operation of the DER intervention. Finally, sensitivity analyses will be performed to assess the impact of future scenarios, considering the planned expansion of DER. This approach will offer critical insights for the future development of the grid, with a focus on high-density urban networks and rural areas with complex configurations. Key performance indicators are as follows.

- **KPI-1** Grid losses (Wh): Grid losses result from difference between energy feed-in and withdrawal.
- **KPI-2** Percentage grid losses (%): Grid losses result from difference between energy feed-in and withdrawal.
- **KPI-3** Reverse power flow (Wh), (min): The reverse power flow represents the injection of energy to the transmission system through the HV/MV transformer.
- **KPI-4** Max power injected to/withdrawn from HV/MV substation (W): Peak power.
- **KPI-5** Grid self-sufficiency (%): Grid self-sufficiency represents the percentage of RES production that is used for supplying the loads and the energy of the loads.
- **KPI-6** Grid self-consumption (%): Grid self-consumption represents the ratio between the RES production used for supplying the loads and the total RES production.
- **KPI-7** Voltage profiles (pu): Voltage profiles can be used to evaluate voltage

stability of the power system.

- **KPI-8** Lines loading factor (pu).
- **KPI-9** Max nadir: Maximum nadir reached during an extreme event (to be defined extreme event)

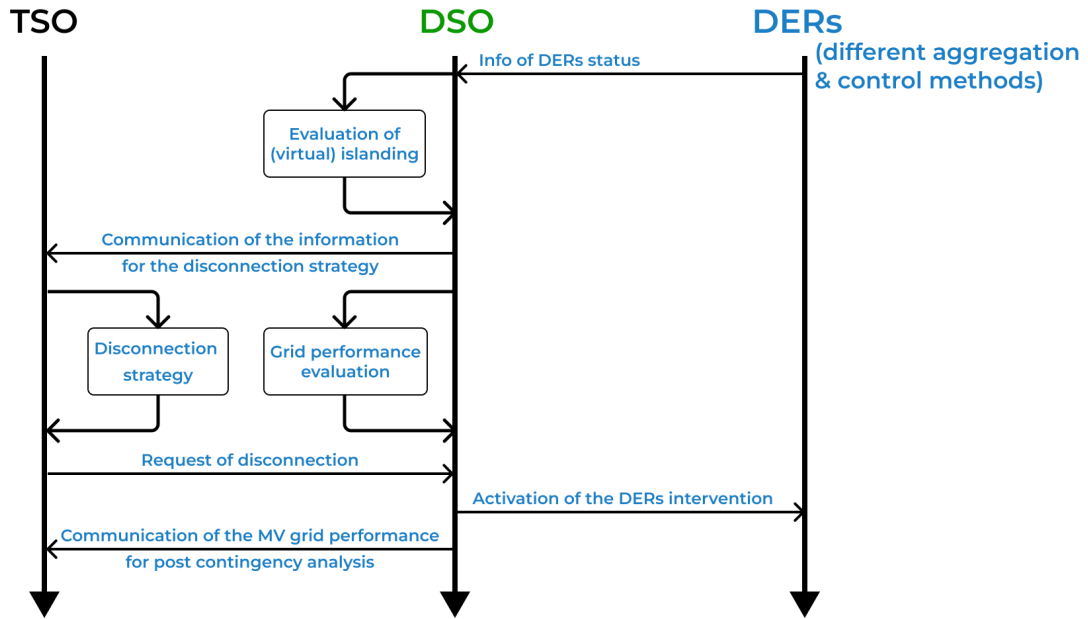


Figure 6.2: Diagram of use case.

It is assumed that the simulated HV network event is able to trigger the Transmission System Operator (TSO) request of support. Prerequisites are:

1. RTS availability for SIL and HIL simulation;
2. software licence (e.g. OPAL RT-Lab, *Matlab/Simulink* etc);
3. availability of network data (both at HV and MV level).

The actors are as follows.

- **Transmission System Operator (TSO):** according to the Article 2.4 of the Electricity Directive 2009/72/EC (Directive): "a natural or legal person responsible for operating, ensuring the maintenance of and, if necessary, developing the transmission system in a given area and, where applicable, its interconnections with other systems, and for ensuring the long-term ability of the system to meet reasonable demands for the transmission of electricity". Moreover, the TSO is responsible for connection of all grid users at the

transmission level and connection of the Distribution System Operator (DSO) within the TSO control area.

- **Distribution System Operator (DSO):** a natural or legal person who is responsible for operating, ensuring the maintenance of and, if necessary, developing the distribution system in a given area and, where applicable, its interconnections with other systems, and for ensuring the long-term ability of the system to meet reasonable demands for the distribution of electricity.
- **Distributed Energy Resources (DER):** DER are defined as energy resources comprised of generation and/or storage and/or controllable load which is connected at the low or medium voltage distribution level. The term “DER” may also indicate a collection of DER units. This collection may also be called a DER plant or a DER facility. In addition, DER plants may act as microgrids. These microgrids may be permanently disconnected from the main grid, but in most cases are normally connected, even though they are designed to disconnect and operate autonomously if necessary.

The exchanged information are:

- **ID1 Voltage** three-phase voltage signal at the HV/MV interface (i.e., at transformer level).
- **ID2 Current** three-phase current signal at the HV/MV interface (i.e., at transformer level).
- **ID3 Apparent power** three-phase apparent power exchanged at the HV/MV interface (i.e., at transformer level).
- **ID4 Frequency** frequency of the transmission system following the grid event.

6.2.2 Use case implementation

At the beginning of the simulation, a 8 MW load step is introduced on the high voltage side of the transformer. This event initiates the under-frequency transient that is the focus of the study.

Feeders 3 and 7 have a high percentage of production linked to their nodes, resulting in an effective power balance contribution to the grid that is approximately zero. Similarly, feeder 4 can be regarded as neutral to the power balance due to its simplicity. The other feeders have to take action in presence of the emergency situation simulated in order to avoid a disconnection from grid by the under frequency relay. In this case study the objective is to evaluate two type of measure that could be considered:

- the load shedding strategy realized with the disconnection of loads by the EAC relays;
- the application of BESS connected to the grid in order to obtain an acceptable transitory without the disconnection of load from the network.

The load shedding strategy is the most straightforward method to maintain frequency stability in the grid. By disconnecting loads in response to a load change, we effectively simulate a generation step, helping to balance the overall power supply. However, this results in a service disruption for the disconnected loads, and once the emergency situation is resolved, the distributor must gradually reconnect the disconnected loads. A sudden reconnection of all loads that were disconnected during the emergency would lead to further emergency situation. The use of BESS is a more costly solution, but it does not require disconnecting users. This strategy differs from load shedding, as it do not aim at the elimination of the load change; instead, it supports generation in responding with a frequency profile that is manageable for the grid, helping to prevent loss of synchronism in the electric generators.

6.3 Results presentation

This section presents the results from the RTS of the model. The mathematical framework introduced in the earlier chapters of this work is now implemented practically using the real-time simulator. The results are aimed at validating the grid model described in Chapter 5, with a focus on the BESS and EAC relay models presented in Sections 5.5 and 5.6, respectively. From an electrical analysis perspective, the frequency stability of the network and the dynamic response of the generator will be highlighted. Additionally, the effectiveness of the proposed approach, specifically the application of EAC relays and the integration of BESS into the grid, will be assessed. The key findings outlined here provide a valuable foundation for further, more detailed studies.

6.3.1 Generator response

The first simulated scenario applies an 8 MW load step to a network without any measures in place to maintain frequency stability (Figure 6.3a). Upon the application of the load step, the generator's rotor slows down, causing the grid frequency to drop and reach a nadir of approximately 49.955 Hz (Figure 6.3b). The dynamic response of the generator (Figure 6.6) results in an increase in mechanical torque. Within about 7.5 seconds, the system stabilizes, returning to a steady-state condition with the grid frequency restored to 50 Hz. The spike in the frequency profile that occurs at the time of the load step can be attributed to a numerical

artifact caused by the sudden change in load conditions as they are not present in the rotor speed profile.

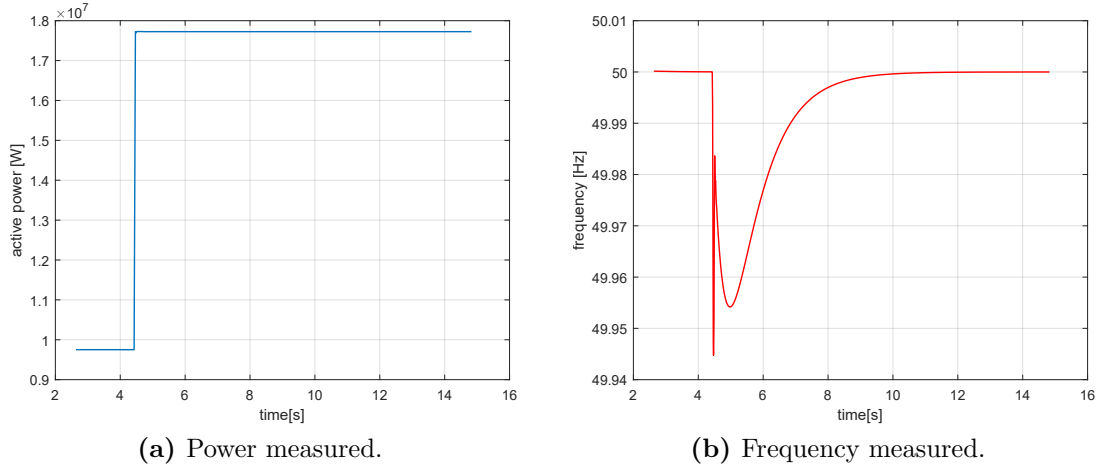


Figure 6.3: Frequency transient in response to an 8 MW load step, without any measures in place to maintain frequency stability.

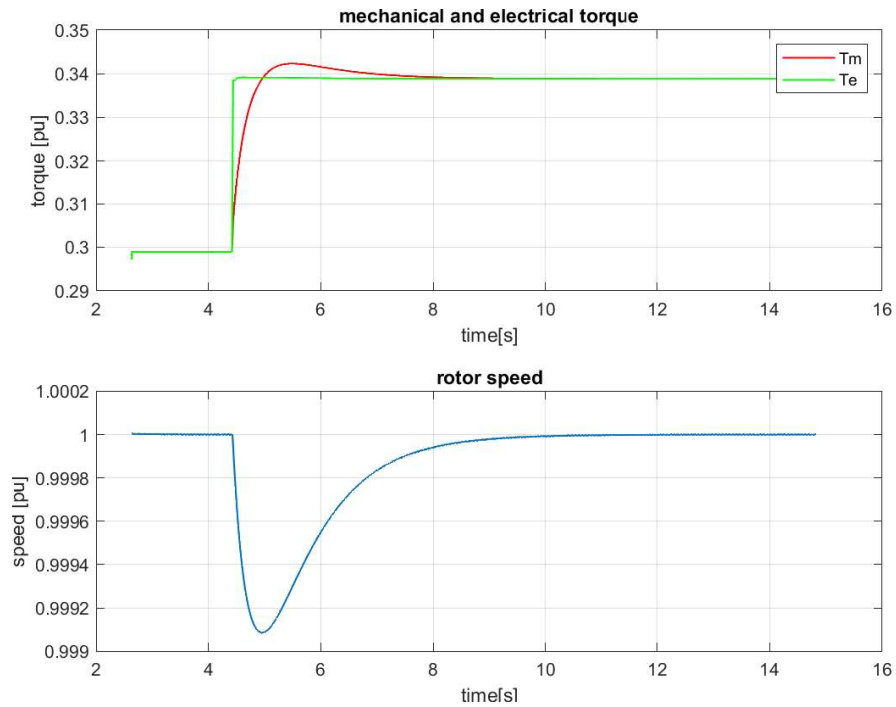


Figure 6.4: Transient in the synchronous generator in response to an 8 MW load step, without any measures in place to maintain frequency stability.

6.3.2 EAC relays action

The EAC relays installed on the network are highlighted with green circles in Figure 5.11. These relays command the disconnection of feeders 1, 2, 5, and 6 from the network, resulting in a virtual generation step of approximately 10 MW. After the 8 MW load step, the EAC relays are triggered by the detection of the under-frequency transient (see figure 6.5a). As a result, the generation must compensate for a -2 MW change in load. During the transient, the frequency drops to a minimum of 49.969 Hz and then overshoots to 50.001 Hz, taking about 6.5 seconds to stabilize before returning to a steady-state condition with the grid frequency restored to 50 Hz (figure 6.5b). The spikes observed in the frequency profile are likely a numerical artifact caused by the abrupt change in load conditions as they are not present in the rotor speed profile.

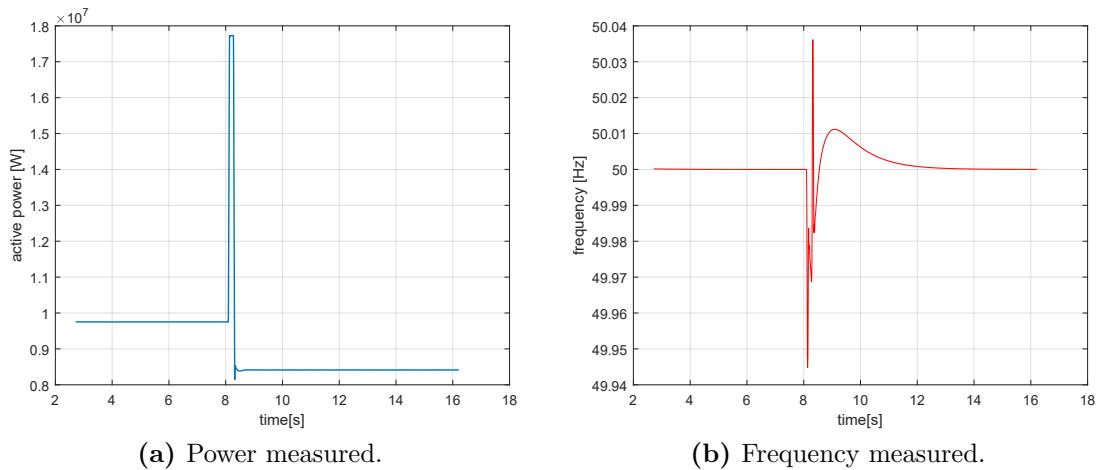


Figure 6.5: Frequency transient in response to an 8 MW load step, with intervention from the EAC relays on feeders 1,2,5 and 6.

In the simulation, the EAC relays are set with a threshold frequency of 49.98 Hz and a time delay of 0.15 seconds, in figure 5.11, the positions of the EAC relays are highlighted with green circles. The relays model is described in section 5.6). It's important to note that disconnecting loads causes service disruptions for users, so the disconnection parameters should be established through contractual agreements directly with them. A further extension of the study should identify the optimal positioning and parametrization of the relays to maximize their positive impact on the network. Moreover, it is essential to implement a strategy that automatically disconnects only the necessary loads to maintain frequency stability, dynamically selecting which loads to disconnect based on the specific emergency situation. The transient at the generation node is particularly noteworthy. The

generator’s regulation must not be disrupted by the initial load step, which can cause excessive oscillations due to the abrupt change in objectives (figure 6.6). This aspect should not be overlooked, and the generator’s regulation connected to the grid should be optimized with this consideration in mind.

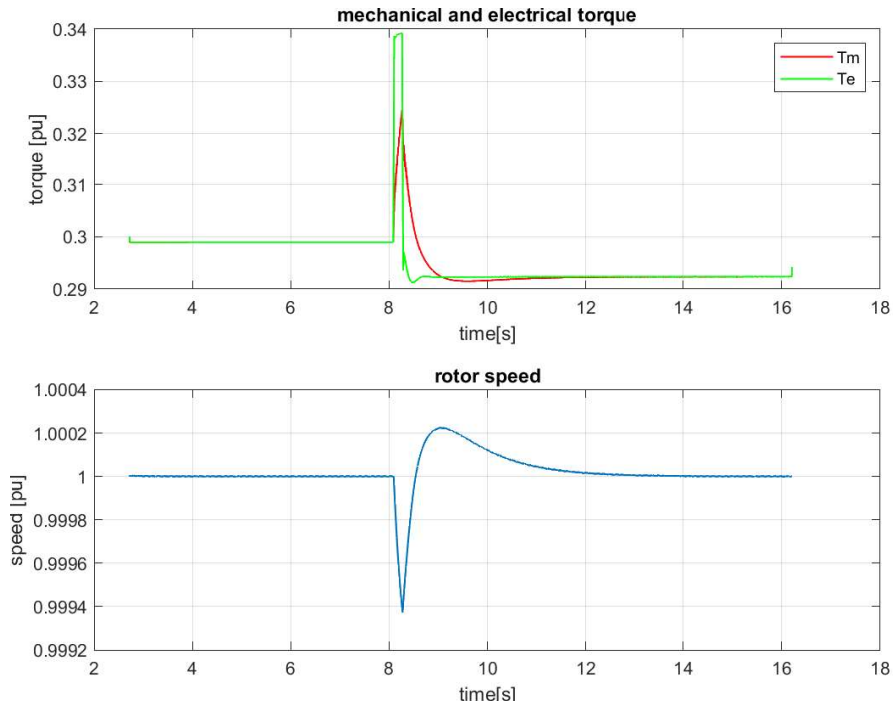


Figure 6.6: Transient in the synchronous generator in response to an 8 MW load step, with intervention from the EAC relays on feeders 1,2,5 and 6.

6.3.3 BESS action

This subsection is divided into several tests, each implementing a different control strategy designed to improve the frequency response. The control and operation strategy of the BESS on the network is more complex than that of the EAC relays, as the BESS does not directly eliminate load. Instead, it should track the transient and supplies power to the grid in the most effective manner. The goal is to achieve a rapid transient response and a minimal frequency nadir. At the beginning of each test, the implemented strategy is described. For better clarity, each BESS is labeled according to the scheme shown in figure 6.7. The BESS units have been positioned on the grid to emulate the load shedding strategy implemented with the EAC relays. Three 1 MW units are connected to feeders 1 and 6, as these feeders each absorb approximately 3 MW, while two 1 MW units are connected to feeders 2 and 5, following the same logic. However, the optimal placement and power

allocation should be explored in greater depth by implementing the Monte Carlo method or other heuristic techniques. At this stage, the goal is to validate the BESS model initially implemented, reflect on potential control issues, and highlight the benefits of this type of solution. The optimization process becomes secondary for now.

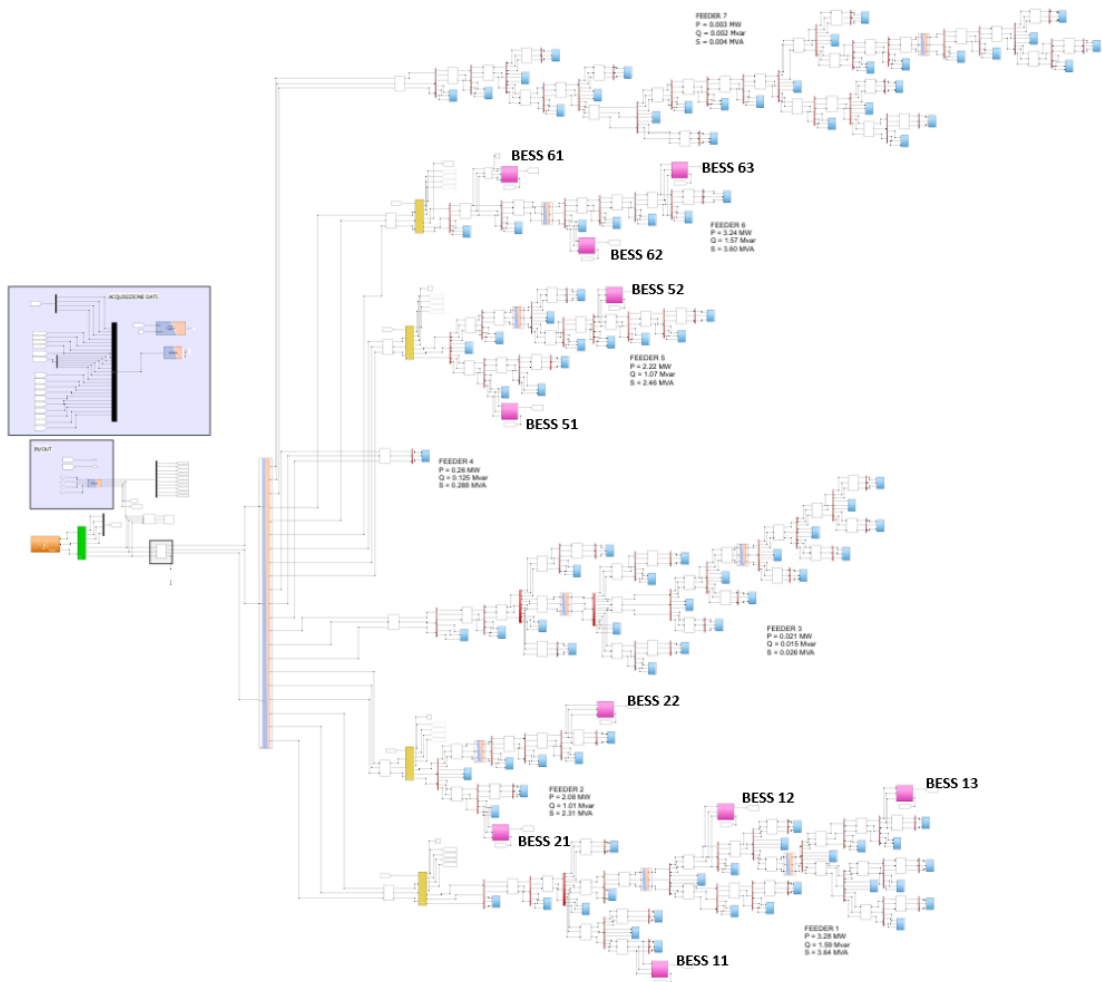


Figure 6.7: BESS installed on the network.

Test 1

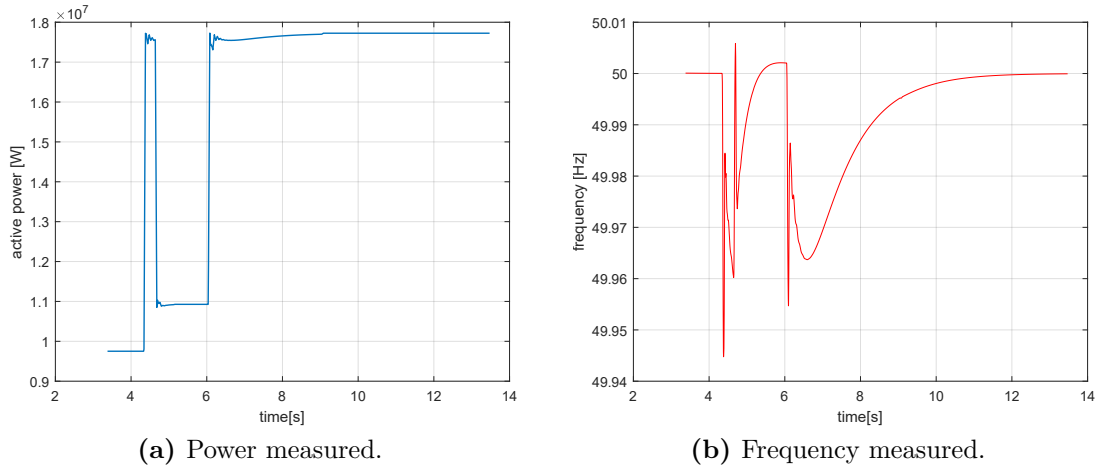


Figure 6.8: Frequency transient in response to an 8 MW load step, with intervention from the BESS - Test 1.

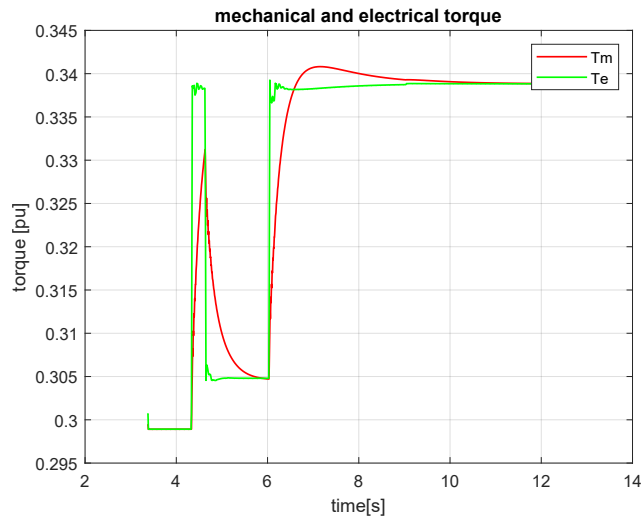


Figure 6.9: Transient in the synchronous generator in response to an 8 MW load step, with intervention from the BESS - Test 1.

In this test, the strategy implemented is the one described in section 5.5. All connected BESS units have the control activated, with each capable of supplying up to 1 MW. The frequency transient reaches a minimum value of 49.960 Hz and restores steady-state conditions within 9.12 seconds (figure 6.8b). The spikes observed in the frequency profile are likely numerical artifacts caused by the abrupt change in load conditions as they are not present in the rotor speed profile. The

frequency transient associated with BESS 12, 13, and 22 does not activate the maximum power output control, as shown in figure 6.10. These units operate solely with droop control. The remaining units supply the grid with 1 MW each at the onset of the transient. This control strategy is suboptimal: it only marginally limits the frequency nadir and the sudden restoration of the load with zero power output from the BESS leads to a secondary transient less severe, but it is still undesirable. Furthermore, such a controlled dynamic causes the generator's regulator to go off track, forcing it to first reduce the torque and then increase it significantly (figure 6.9). A good control system would not require this waste of energy from the generation process, the optimal control must be able to maintain the frequency without setting a false objective for the generator governor.

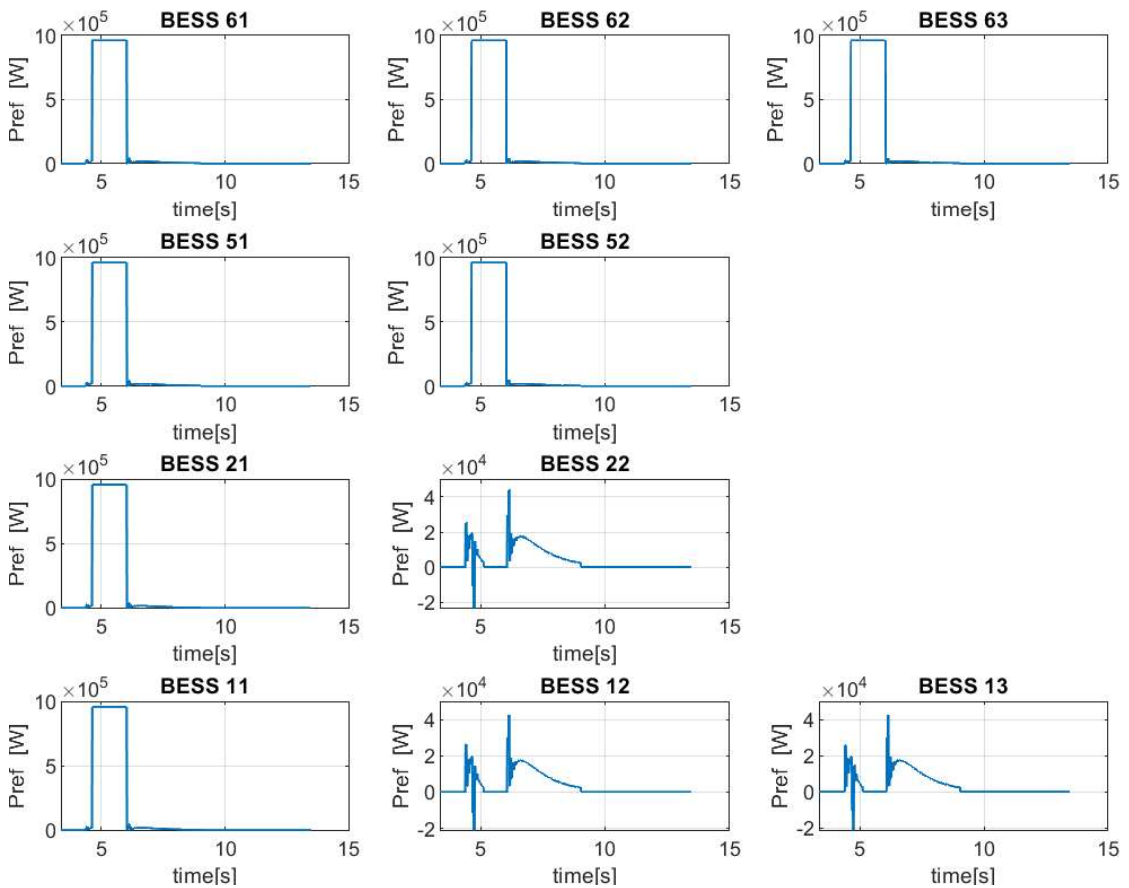


Figure 6.10: Action of BESS connected to the network in response to an 8 MW load step - Test 1.

Test 2

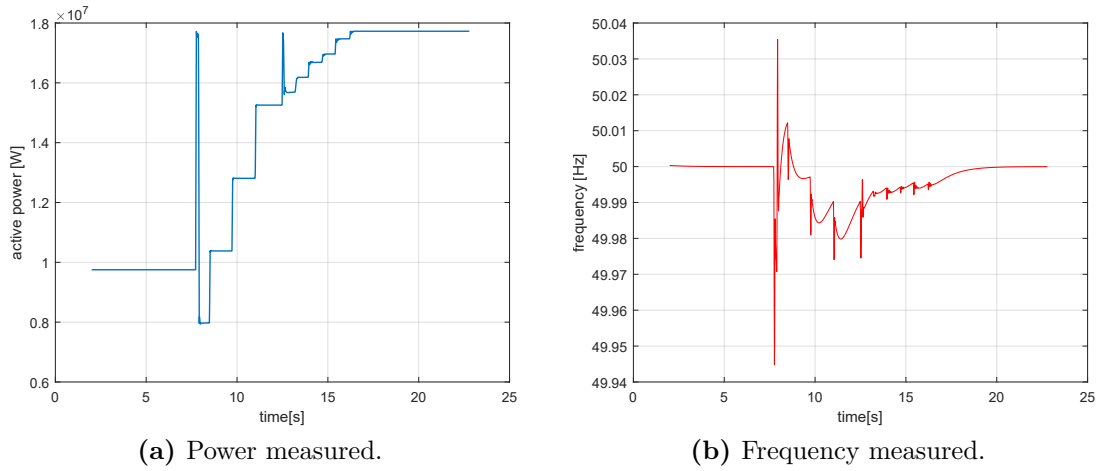


Figure 6.11: Frequency transient in response to an 8 MW load step, with intervention from the BESS - Test 2.

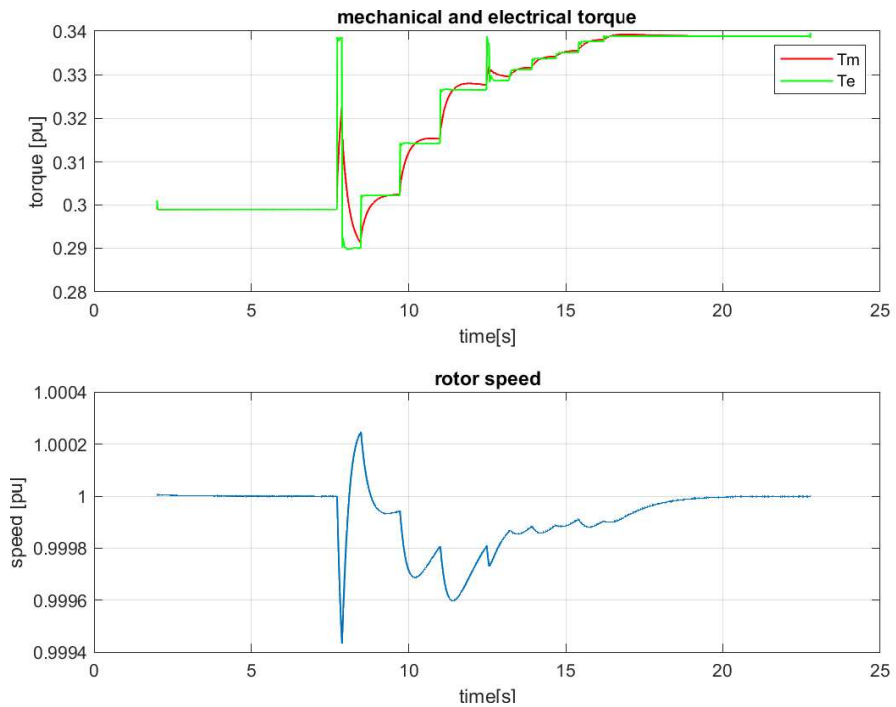


Figure 6.12: Transient in the synchronous generator in response to an 8 MW load step, with intervention from the BESS - Test 2.

In this test, the BESS control was modified to implement a four-step disconnection process for each BESS, aiming to limit the second transient observed in Test 1. The control command progresses to the next step after detecting a $ROCOF > 0$ for 0.2 seconds and a frequency greater than $f_{ter} = 49.99$ Hz. All available BESS units have their control activated, and at the start of the transient, they each supply all the power they have available. The innovation in the control strategy lies in the disconnection transient, which can be seen in figure 6.13. This approach gradually reintroduces the total load to the HV network, so the generation does not immediately supply the entire load step. Instead, the load is redistributed over time (figure 6.12). It is important to note the total reactivation of BESS 13 and 22 towards the end of the transient, this is not ideal as it causes an unnecessary extension of the frequency transient. This issue will be addressed in subsequent tests. Despite a longer transient compared to the others, 13.69 seconds, the frequency nadir only reaches 49.971 Hz with an overshoot of 50.012 Hz.

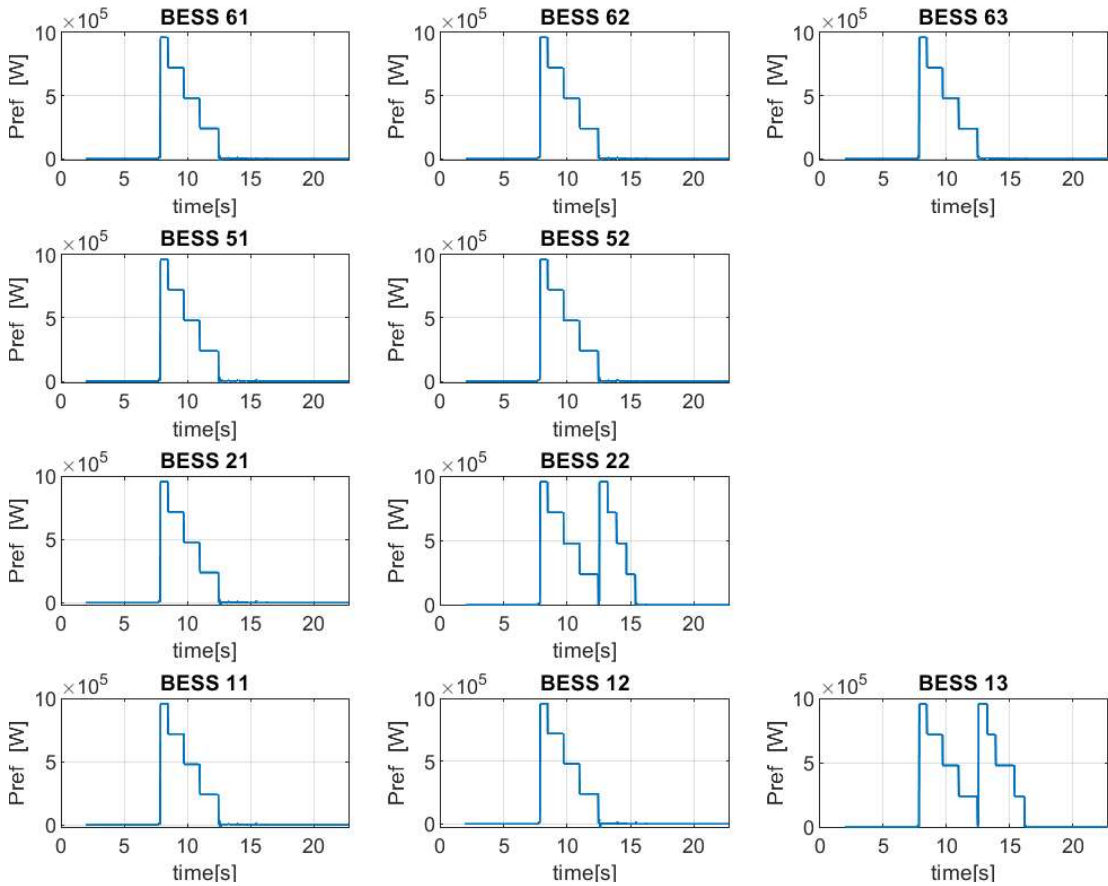


Figure 6.13: Action of BESS connected to the network in response to an 8 MW load step - Test 2.

Test 3

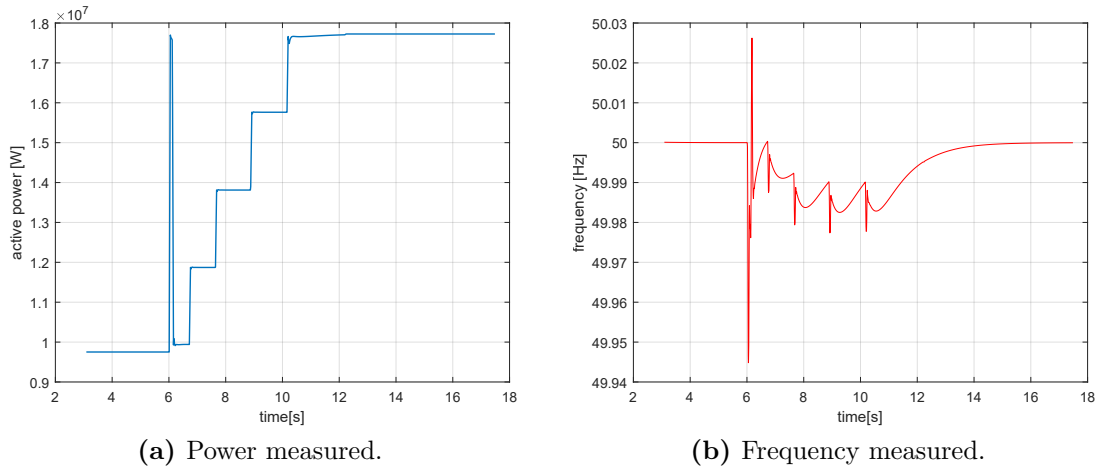


Figure 6.14: Frequency transient in response to an 8 MW load step, with intervention from the BESS - Test 3.

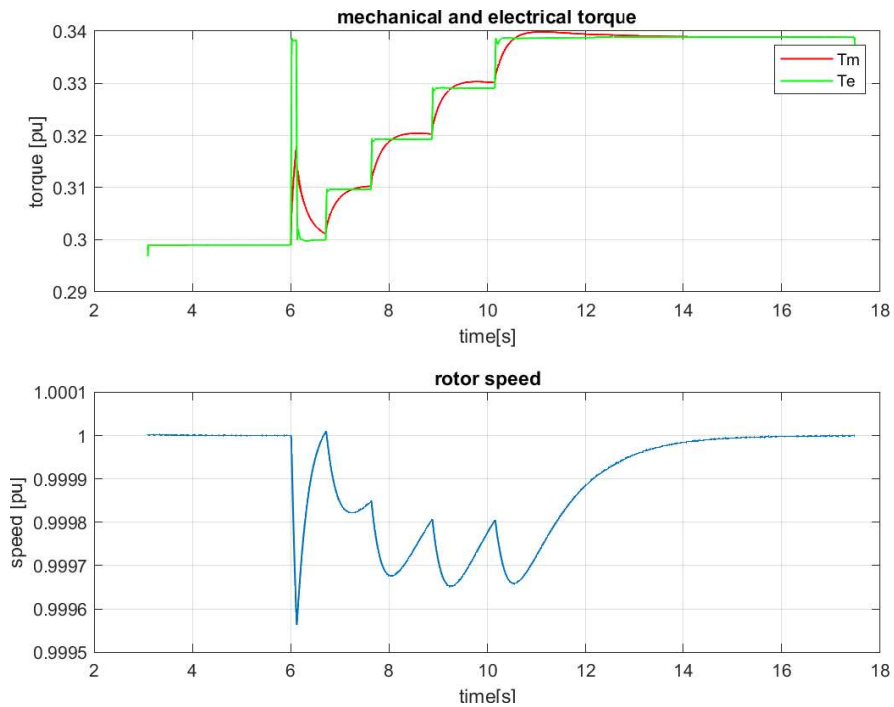


Figure 6.15: Transient in the synchronous generator in response to an 8 MW load step, with intervention from the BESS - Test 3.

In this test the control of BESS 13 and 22 is not activated, the control strategy implemented on the activated units is the same described in Test 2. The intervention of active BESS is similar at the one already seen in the precedent test (figure 6.16) but, here, the available power to supply the frequency transient correspond exactly to the load step that the network have to bear. In this scenario the frequency nadir is about 49.976 Hz, there is no frequency overshoot and the steady-state condition is reached in 10.79 seconds (figure 6.11b). Similarly, the spikes observed in the frequency profile are likely numerical artifacts caused by the abrupt change in load conditions as they are not present in the rotor speed profile. An interesting observation is the transient behavior of the mechanical and electrical torques, shown in figure 6.15. The combined action of the BESS actively connected to the network allows for control of the electrical torque, as it corresponds to the electrical power demanded by the generating node, and consequently, enables control over the mechanical transient experienced by the generator.

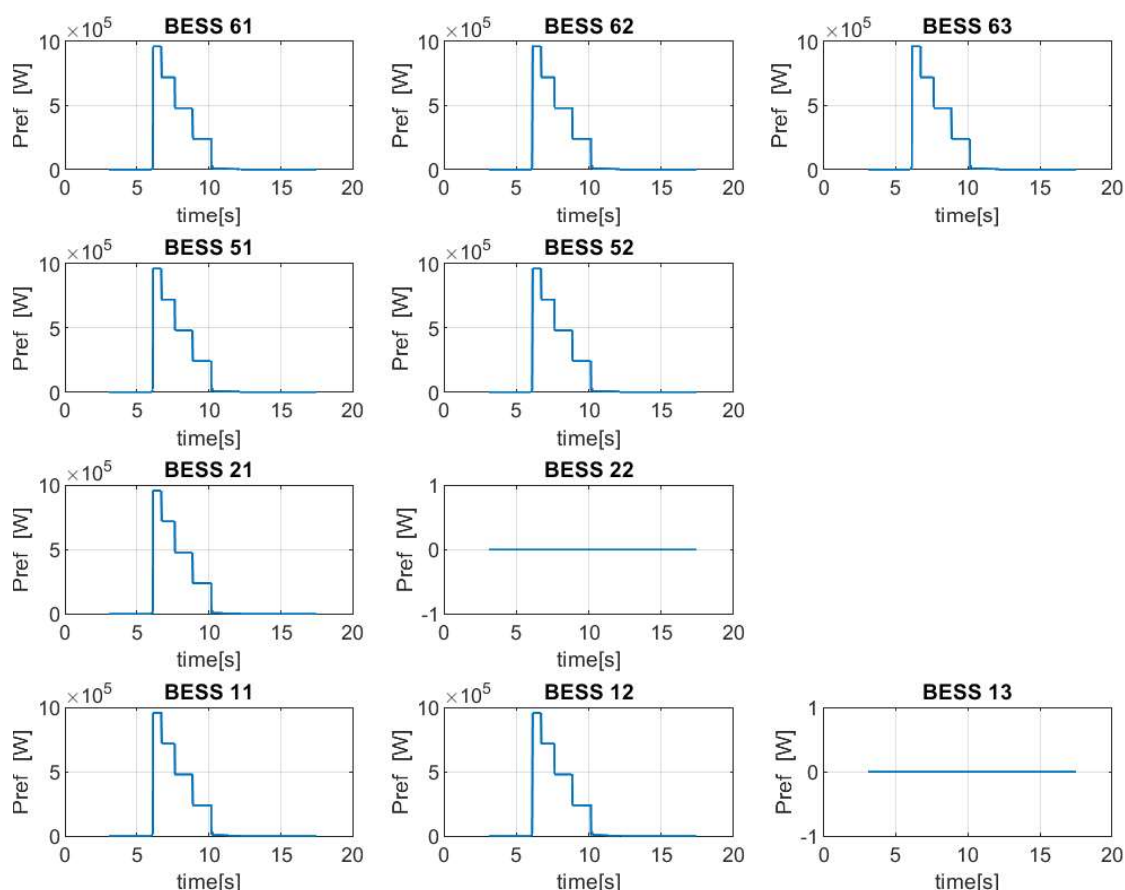


Figure 6.16: Action of BESS connected to the network in response to an 8 MW load step - Test 3.

Test 4

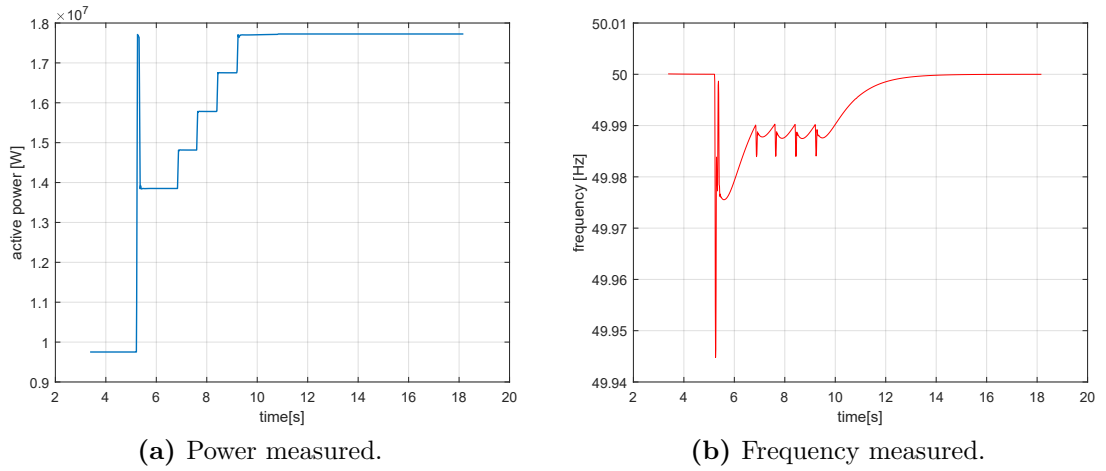


Figure 6.17: Frequency transient in response to an 8 MW load step, with intervention from the BESS - Test 4.

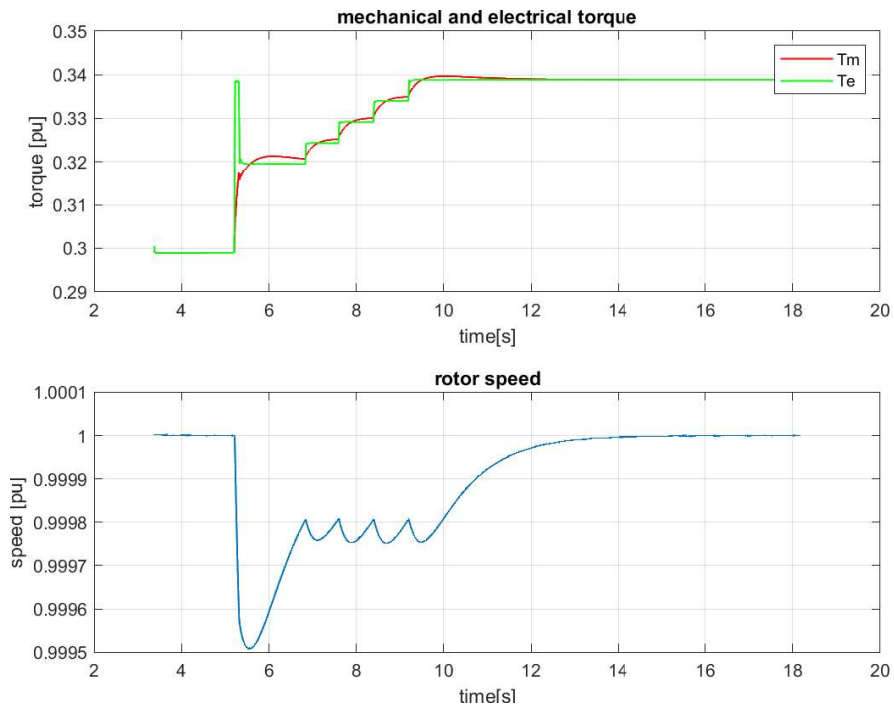


Figure 6.18: Transient in the synchronous generator in response to an 8 MW load step, with intervention from the BESS - Test 4.

In this test, only the controls of BESS 11, 21, 51, and 61 are activated, using the control logic presented in Test 2, providing a total of 4 MW to support the frequency transient. The nadir frequency is around 49.975 Hz, with no frequency overshoot, and the transient lasts for 10.04 seconds (Figure 6.17b). As with the other tests, the spikes observed in the frequency profile are likely numerical artifacts caused by the abrupt change in load conditions as they are not present in the rotor speed profile. The result is not immediately obvious, as it might seem that with less available power, the frequency profile could still improve. This is because, as previously discussed, the role of the BESS is not to eliminate load but to assist the generating node during the transient by shaping an optimal torque profile for the mechanical system.

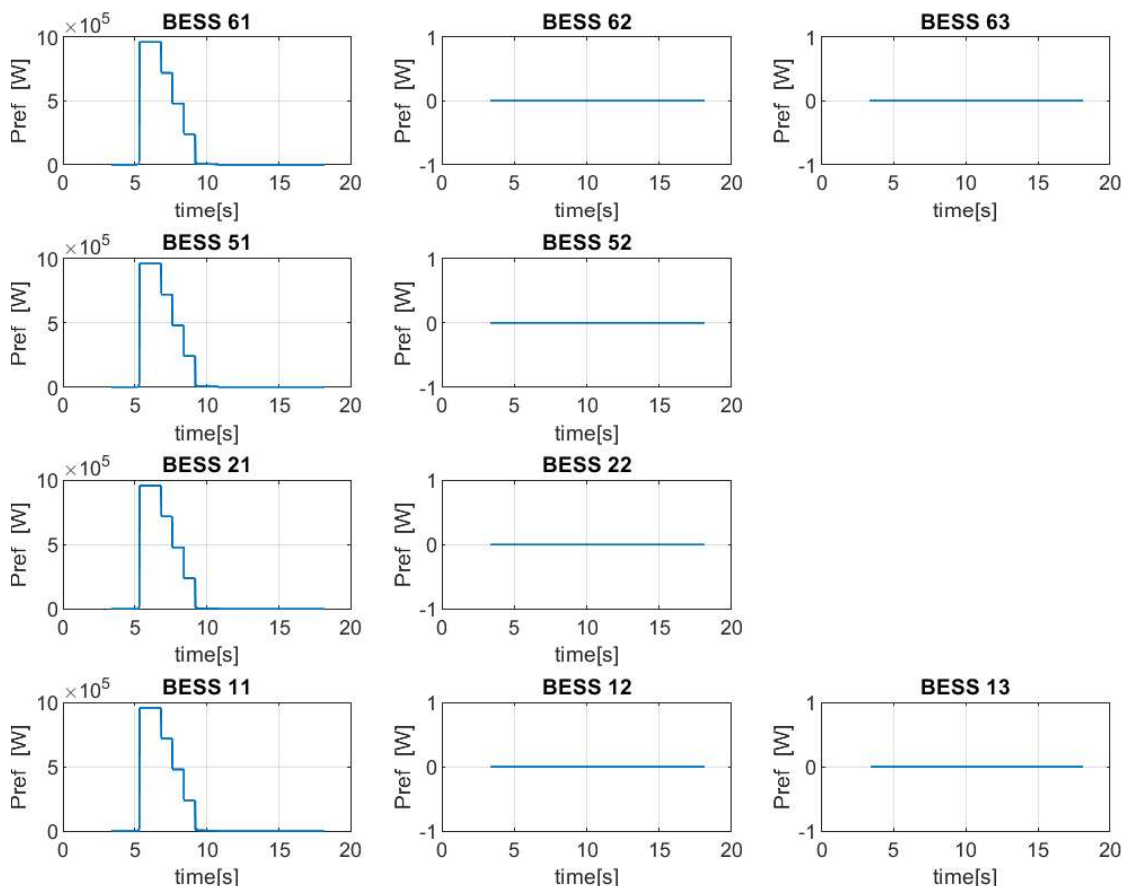


Figure 6.19: Action of BESS connected to the network in response to an 8 MW load step - Test 4.

Referring to Figure 6.18, it is clear that when the BESS are activated, they are controlled in such a way as to match the electrical torque with the mechanical

torque at that moment. Unlike in previous tests, here the mechanical torque does not need to be significantly reduced before starting to increase again. Instead, the BESS action is well-tuned to the generator's regulation at the moment of intervention. This synchronization is the key strength of this strategy.

6.3.4 Summary of simulation results

The table below summarizes the main characteristics of the frequency profiles observed following the 8 MW load step, based on the different strategies implemented in the previous sections, to facilitate a comparison of the effectiveness of each strategy.

Simulation	Nadir [Hz]	Overshoot [Hz]	Duration [s]
Generator response	49.950	no	7.5
EAC action	49.969	50.001	6.5
BESS action (Test 1)	49.960	50.002	9.12
BESS action (Test 2)	49.971	50.012	13.69
BESS action (Test 3)	49.976	no	10.79
BESS action (Test 4)	49.975	no	10.04

Table 6.2: Summary of frequency profile obtained.

Chapter 7

Conclusion and future works

This thesis has examined the critical role and potential of real-time simulation for the effective management and optimization of distribution grids. As the energy sector advances with increasing integration of RES, ESS, and decentralized power generation, traditional grid management approaches face new challenges. Real-time simulation offers grid operators a powerful tool to test strategies, optimize configurations, and enhance grid reliability and resilience without risking real-world power outages.

The real-time simulation model developed in this study demonstrates how modern distribution grids can be effectively modeled and tested, enabling a detailed analysis of their behavior under various operational scenarios. This approach allows for evaluating control strategies, assessing the performance of distributed energy resources, and improving decision-making processes in operational contexts.

The simulation results validate the distribution grid model, with a focus on the BESS and EAC relay models. From an electrical analysis perspective, the proposed approach — specifically, the integration of BESS units into the grid — demonstrates its effectiveness in enhancing frequency stability. The BESS provides a viable strategy to support frequency control, minimizing the need for load shedding and thereby reducing service disruptions for users. By optimizing control logic, this approach mitigates the frequency nadir, resulting in a less pronounced frequency dip and a smoother transient response. This response, in turn, alleviates the load on the generation node, contributing to a more stable and resilient grid during frequency fluctuations.

While this thesis presents a solid foundation for real-time simulation in distribution networks, it also highlights areas for future research and development. Future applications of the model could focus on analyzing frequency variations and the

integration of variable RES. Further refinement of the model, such as the incorporation of more detailed physical models, enhanced optimization techniques, and integration with real-world hardware systems, could provide even more accurate simulations and allow for more advanced testing environments like Hardware in the Loop simulations.

As the energy transition accelerates, the need for tools that can simulate, analyze, and optimize distribution grid performance in real-time becomes even more pressing. The work presented in this thesis contributes to the growing body of knowledge in this field, offering a stepping stone toward smarter, more resilient electrical grids that can effectively integrate renewable energy sources and meet the demands of the future.

Bibliography

- [1] John Denholm Lambert et al. *Numerical methods for ordinary differential systems*. Vol. 146. Wiley New York, 1991 (cit. on pp. 10, 15).
- [2] C William Gear. «Numerical initial value problems in ordinary differential equations». In: *Prentice-Hall series in automatic computation* (1971) (cit. on pp. 10, 15).
- [3] A.Benigni A.Monti. *Modeling and Simulation of Complex Power Systems*. HBK, 2022 (cit. on pp. 16–18, 20, 36).
- [4] O. Wasynczuk and S.D. Sudhoff. «Automated state model generation algorithm for power circuits and systems». In: *IEEE Transactions on Power Systems* 11.4 (1996), pp. 1951–1956. DOI: 10.1109/59.544669 (cit. on p. 23).
- [5] Jean Bélanger, Philippe Venne, and Jean-Nicolas Paquin. «The what, where and why of real-time simulation». In: *Planet Rt* 1.1 (2010), pp. 25–29 (cit. on p. 25).
- [6] Hermann W Dommel. «Digital computer solution of electromagnetic transients in single-and multiphase networks». In: *IEEE transactions on power apparatus and systems* 4 (1969), pp. 388–399 (cit. on p. 29).
- [7] Jean Bélanger, Amine Yamane, Andy Yen, Sébastien Cense, and Pierre-Yves Robert. «Validation of eHS FPGA reconfigurable low-latency electric and power electronic circuit solver». In: *IECON 2013-39th Annual Conference of the IEEE Industrial Electronics Society*. IEEE. 2013, pp. 5418–5423 (cit. on p. 33).
- [8] Pau Marti, Josep M Fuertes, Gerhard Fohler, and Krithi Ramamritham. «Jitter compensation for real-time control systems». In: *Proceedings 22nd IEEE Real-Time Systems Symposium (RTSS 2001)(Cat. No. 01PR1420)*. IEEE. 2001, pp. 39–48 (cit. on p. 36).
- [9] Federico Milano, Florian Dörfler, Gabriela Hug, David J Hill, and Gregor Verbič. «Foundations and challenges of low-inertia systems». In: *2018 power systems computation conference (PSCC)*. IEEE. 2018, pp. 1–25 (cit. on p. 39).

- [10] Mattia Gangi. «Dynamic Modelling of Virtual and Real Inertia Systems in Green Microgrids». MA thesis. Politecnico di Torino, 2021 (cit. on pp. 39, 40).
- [11] Fabrizio Pilo, Giuditta Pisano, Sandra Scalari, Diego Dal Canto, Alfredo Testa, Roberto Langella, Roberto Caldon, and Roberto Turri. «ATLANTIDE-Digital archive of the Italian electric distribution reference networks». In: *IET* (2012) (cit. on p. 41).
- [12] Woo Yeong Choi, Kyung Soo Kook, and Ga Ram Yu. «Control strategy of BESS for providing both virtual inertia and primary frequency response in the Korean power system». In: *Energies* 12.21 (2019), p. 4060 (cit. on p. 49).
- [13] Amine Yamane, Simon Abourida, Yahia Bouzid, and François Tempez. «Real-time simulation of distributed energy systems and microgrids». In: *IFAC-PapersOnLine* 49.27 (2016), pp. 183–187 (cit. on p. 54).
- [14] *ARTEMIS User Guide*, available on: <http://www.opal-rt.com>. (Cit. on p. 54).
- [15] Simon Abourida, Christian Dufour, and Jean Bélanger. «Real-Time and Hardware-In-The-Loop Simulation of Electric Drives and Power Electronics: Process, problems and solutions». In: *Proceedings of the International Power Electronics Conference (IPEC-Niigata 2005)*, Niigata, Japan. 2005, pp. 4–8 (cit. on p. 55).
- [16] *OPAL-RT OP5700 User guide*, available on: <https://www.opal-rt.com/resource-center/document/?resource=L001610337> (cit. on pp. 55, 56).